

AN ABSTRACT OF THE THESIS OF

CHIH CHING SHIH for the degree of MASTER OF SCIENCE  
in CHEMICAL ENGINEERING presented on March 6, 1978  
Title: OXYGEN ABSORPTION IN BRINE AS A RESULT OF A PLUNGING JET.  
Abstract approved: Redacted for privacy

Charles E. Wicks

A mathematical model is developed to study the rate of absorption of oxygen as a result of a plunging jet. A 'closed' system with recycle stream was used to reduce the complexity of the mass transfer process in the plunging jet system.

The summation of the product of the mass transfer coefficient and interfacial area over all the entrained bubbles, the transfer factor (TF), is found to be proportional to the product of jet stream  $N_{Re}$  and  $N_{We}$  in various solutions.

Also, the TF is found to be proportional to the concentration of sodium chloride in the solution. On the other hand, the rate of absorption of oxygen reaches a maximum value as the concentration of sodium chloride increases. Then the rate of absorption decreases gradually.

The formation of very many tiny bubbles in a solution will increase the interfacial area substantially. And the turbulency of a solution depends on the mobility of the solvent molecules. Hence, the hydrodynamic situation of the solution plays an important role in rate of absorption. In other words, the inter-molecular structure determines the change in TF.

Other aspects, the jet length and impurities are found to be important in rate of absorption in a plunging jet system.

Oxygen Absorption in Brine as a Result  
of a Plunging Jet

by

Chih Ching Shih

A THESIS

submitted to

Oregon State University

in partial fulfillment of  
the requirements for the  
degree of

Master of Science

Commencement June 1978

APPROVED:

**Redacted for privacy**

---

Professor of Chemical Engineering  
in charge of major

**Redacted for privacy**

---

Head of Chemical Engineering Department

Redacted for privacy

---

Dean of Graduate School

Date thesis is presented March 6, 1978

Typed by CAMPUS PRINTING & COPY CENTER for CHIH CHING SHIH

## ACKNOWLEDGEMENT

First, I would like to thank Dr. C. E. Wicks for his advice, guidance, and continued interest in this work.

I would like to express my appreciation to Dr. H. Freund, Dr. S. J. Hawkes and Dr. R. V. Mrazek for their helpful suggestions.

Thanks to Mr. Lii-ping Leu, my best friend in Oregon, for his extensive criticism which results in an early completion of this work.

I would like to thank National Council for Steam Improvement which lent me the oxygen electrode.

I am grateful to Gayla, my fiancée, for her encouragement and comfort during this work. Her LTC plays an important role in my work.

Last but not least, thanks to all my friends for their fruitful advices.

To  
Gayla



JC

## TABLE OF CONTENTS

INTRODUCTION	1
THEORY	3
EXPERIMENTAL EQUIPMENT AND PROCEDURE	7
General Description	7
Procedure	14
DISCUSSION	17
CONCLUSION	35
RECOMMENDATIONS	37
NOMENCLATURE	38
BIBLIOGRAPHY	40
APPENDICES	
Appendix I: Experimental Code	42
Appendix II: Equipment and Material Specification	43
Appendix III: Experimental Data	44
Appendix IV: Sample Calculations	76

## LIST OF ILLUSTRATIONS

<u>Figure</u>	<u>Page</u>
1. Tap-water and pool.	2
2. Details of absorption pool.	9
3. Schematic diagram of absorption pool.	10
4. Study of total transfer factor (top) and surface transfer factor (bottom).	13
5. Comparison between Hauxwell (8) correlation and correlation of this work.	18
6. Bubbles penetration depth. Jet length = 90 mm (left) Jet length = 25 mm (right).	19
7. The TF for oxygen absorption in brine (1%).	21
8. The TFS for oxygen absorption in brine (1%).	22
9. The TF for oxygen absorption in brine (5%).	23
10. The TF for oxygen absorption in different solutions.	24
11. Structure of water molecule. From Morrison and Boyd (13).	26
12. The structure of ionic solution. From Horne (9).	27
13. Oxygen bubbles in different solvents. Water (left). Brine, 5% (right).	30
14. Comparison of rate of absorption.	32
15. Amount of bubbles attached to the cylinder wall in different solvents. Water (left). Brine, 5% (right).	33

## LIST OF TABLES

<u>Table</u>	<u>Page</u>
1. Jet tube dimensions.	7
2. Experimental jet conditions with water as solvent.	11
3. Experimental jet conditions with brine (1%) as solvent.	11
4. Experimental jet conditions with brine (5%) as solvent.	12
5. Comparison of the rate of absorption.	31

# OXYGEN ABSORPTION IN BRINE AS A RESULT OF A PLUNGING JET

## INTRODUCTION

A common phenomenon of air entrainment due to a plunging jet can be observed both in nature and in daily life. A waterfall and a stream of tap-water entrain a fair amount of air bubbles into the pool. The increased interfacial area between air bubbles and water as a result of a plunging jet is very beneficial for water aeration. However, air entrainment is a common problem in some industries when the air bubbles are not desired.

From energy stand-point, a plunging jet is more favorable than common mechanical devices, such as an agitator, in certain aspects. The great interfacial area between bubbles and solvent as well as the turbulence caused by a plunging jet increases the aeration capacity. The application of this phenomenon in industries, especially in wastewater treatment, may be promising.

It is extremely difficult to understand the actual mass transfer process in this complex plunging jet system. However, a simplified system is used to study the mass transfer process.

The objective of this work is to study the mass transfer process between oxygen and brine as a result of a plunging jet.

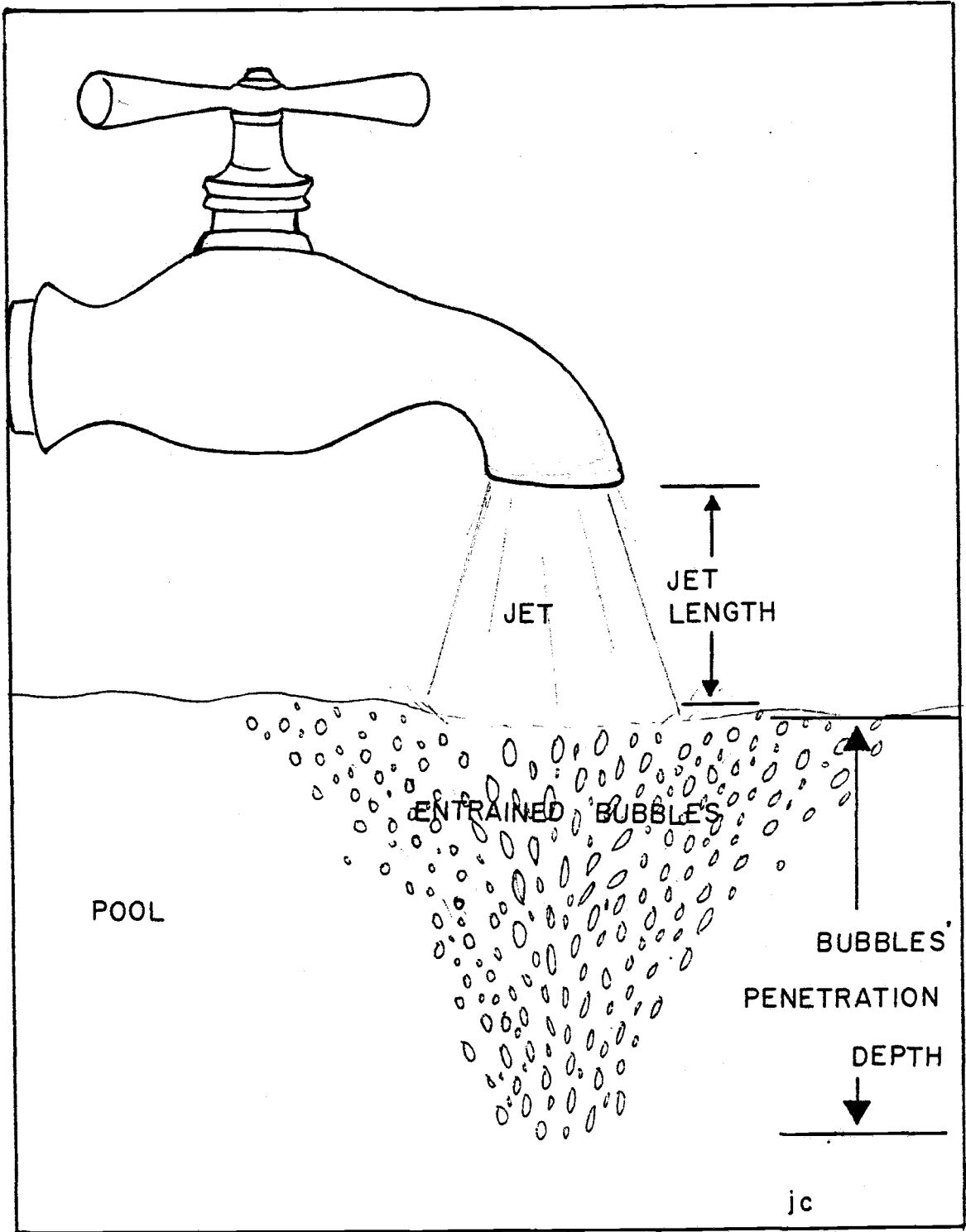


FIGURE 1. Tap-water and pool.

## THEORY

As a matter of preference, the following section will use the symbols designated by Welty, Wicks and Wilson (24). A great effort has been made to avoid any unnecessary confusion because of differences in notations.

Consider the absorption pool as a control volume. The oxygen is absorbed by the solvent in four different aspects: (1) through the jet stream surface; (2) through the pool surface; (3) through the surface of entrained bubbles; (4) and from the oxygen content in the inlet stream. This amount of input oxygen will either be accumulated in the absorption pool or carried out by the exit stream. A material balance for oxygen in the control volume gives:

$$\frac{d(C_L V)}{dt} = W_J + W_S + W_B + Q_I C_I - Q_E C_E \quad (1)$$

where

- $C_E$  = oxygen concentration in the exit stream.
- $C_I$  = oxygen concentration in the inlet stream.
- $C_L$  = oxygen concentration in the pool.
- $Q_E$  = volumetric flow rate of exit stream.
- $Q_I$  = volumetric flow rate of inlet stream.
- $t$  = time
- $W_B$  = rate of absorption through the entrained bubble surface.

$W_J$  = rate of absorption through the jet surface.

$W_S$  = rate of absorption through the pool surface.

The equation can be simplified if one can assume a constant-pool volume, a perfectly mixed tank and negligible rate of absorption through the jet surface. With a 'closed system' which involves a recycle stream flowing rapidly through a short recycle line, the following relationships will hold:

$$C_L = C_E = C_I \quad (2)$$

$$W_J = 0 \quad (3)$$

$$Q_E = Q_I \quad (4)$$

Substituting Equations (2), (3), and (4) into Equation (1) one obtains:

$$V \frac{dC_L}{dt} = W_S + W_B \quad (5)$$

The Whitman two film theory is used to describe the rate of absorption through the pool surface. The expression is as follows:

$$W_S = K_{LS} A_S (C^* - C_L) \quad (6)$$

where

$K_{LS}$  = overall mass transfer coefficient (surface).

$A_S$  = surface area of absorption pool.

$C^*$  = concentration of oxygen in equilibrium with the gaseous atmosphere.

The same theory is used to describe the rate of absorption through bubble surface. For some jth bubble,

$$W_{Bj} = k_{Lj} A_j (C_{ij} - C_L) \quad (7)$$

where

$k_{Lj}$  = liquid film mass transfer coefficient for  $j$ th bubble.

$A_j$  = surface area of  $j$ th bubble.

$C_{ij}$  = boundary concentration at the gas-liquid interface.

Upon summing up all of the  $n$  entrained bubbles and again using the overall mass transfer coefficient, the following equation is obtained,

$$W_B = \sum_{j=1}^n k_{Lj} A_j (C^* - C_L) \quad (8)$$

For simplicity, the concept of a transfer factor, TF, is used to represent the product of the mass transfer coefficient and surface area. This idea has been used successfully by Jackson (10) and Hauxwell (8).

Let

$$TF = \sum_{j=1}^n k_{Lj} A_j \quad (9)$$

$$TFS = K_{LS} A_S \quad (10)$$

and

$$TTF = TFS + TF \quad (11)$$

If one substitute Equations (7), (8), (9), and (10) into Equation (5), the following expression is obtained.

$$V \frac{dC_L}{dt} = TFS (C^* - C_L) + TF (C^* - C_L) \quad (12)$$

Equation (12) is divided by  $VC^*$  to get the dimensionless concentration,  $C^+$ . The equation reduces to:

$$\frac{dC^+}{dt} = \left(\frac{TTF}{V}\right) (1 - C^+) \quad (13)$$

If one assumes that TTF is not a function of concentration nor time, the integration of Equation (13), with the initial condition  $C^+ = C_0^+$  at  $t = 0$ , gives:

$$\ln \left[ \frac{1 - C_0^+}{1 - C^+} \right] = \left(\frac{TTF}{V}\right) t \quad (14)$$

For simplicity, let

$$z = \left[ \frac{1 - C_0^+}{1 - C^+} \right] \quad (15)$$

Then

$$\ln (z) = \left(\frac{TTF}{V}\right) t \quad (16)$$

Equation (16) indicates a linear relationship between  $\ln (z)$  and  $t$  through the origin with the slope equal to  $TTF/V$ . If  $TF = 0$ , Equation (16) reduced to

$$\ln (z) = \left(\frac{TFS}{V}\right) t \quad (17)$$

Equation (11), (16) and (17) are used to find the TF as a function of jet characteristics.

## EXPERIMENTAL EQUIPMENT AND PROCEDURE

General Description

A 438 mm ID glass cylinder, about 380 mm high, was placed between two 12 mm plastic plates. Gaskets and silicon were used to provide proper seatings. A pool depth of 270 mm was chosen such that the depth was sufficient to contain all of the entrained bubbles from the jets.

The jet nozzle was placed at the center of the cylinder cover. The nozzle fitting was designed such that the jet nozzle was interchangeable; the jet nozzle could be raised and lowered at will. The nozzles were made from stainless steel tubing; each has different length to ensure a fully developed velocity profile. The diameter and L/D ratio of the nozzles are tabulated in Table 1.

TABLE 1. Jet tube dimensions.

Jet	Diameter (mm)	L/D
S	2.25	136
M	5.40	92
L	6.80	64

Sampling of the pool content was an important role in every run and care was taken to avoid sample contamination. Three 1/8-in. OD stainless steel tubing located at 154, 51 and 102 mm from the center are designated as sample A, B, and C. The corresponding sample points

were located at 220, 152 and 64 mm from the bottom of the cylinder. A fourth location, designated as sample D, was located inside the pool exit line. Details of the enclosed cylinder, nozzle and sample points are illustrated in Figure 2.

A heat exchanger was used to maintain the fluid at the desired temperature. A pump incorporated with a rotameter was used to adjust the flow rate of the recycle stream. Polyethylene tubings were used for appropriate connections in the system.

Brine was supplied to the enclosed cylinder from a preparation tank. A 60-litre polyethylene tank, equipped with a stirrer and submersion heaters, were used in the preparation of brine. This tank was placed at a higher level with respect to the cylinder. The fluid flowed directly into the cylinder whenever the valve was opened.

Compressed oxygen was fed through a regulator and then bubbled through water to insure its saturation. Water-saturated oxygen was then fed into the enclosed cylinder. The pressure of the gas inside the cylinder was controlled by an adjustable, submerged bubble device. The vapor pressure was measured by a water manometer. The schmatic diagram is illustrated in Figure 3.

Gal-Or, Hauck and Hoelscher (6) indicated that a slight 'contamination' of the 'pure' fluid in the system affects the transfer coefficient significantly. Tap-water was expected to be more realistic than distilled-water. Hence, tap-water was used to make the brine solutions throughout this work.

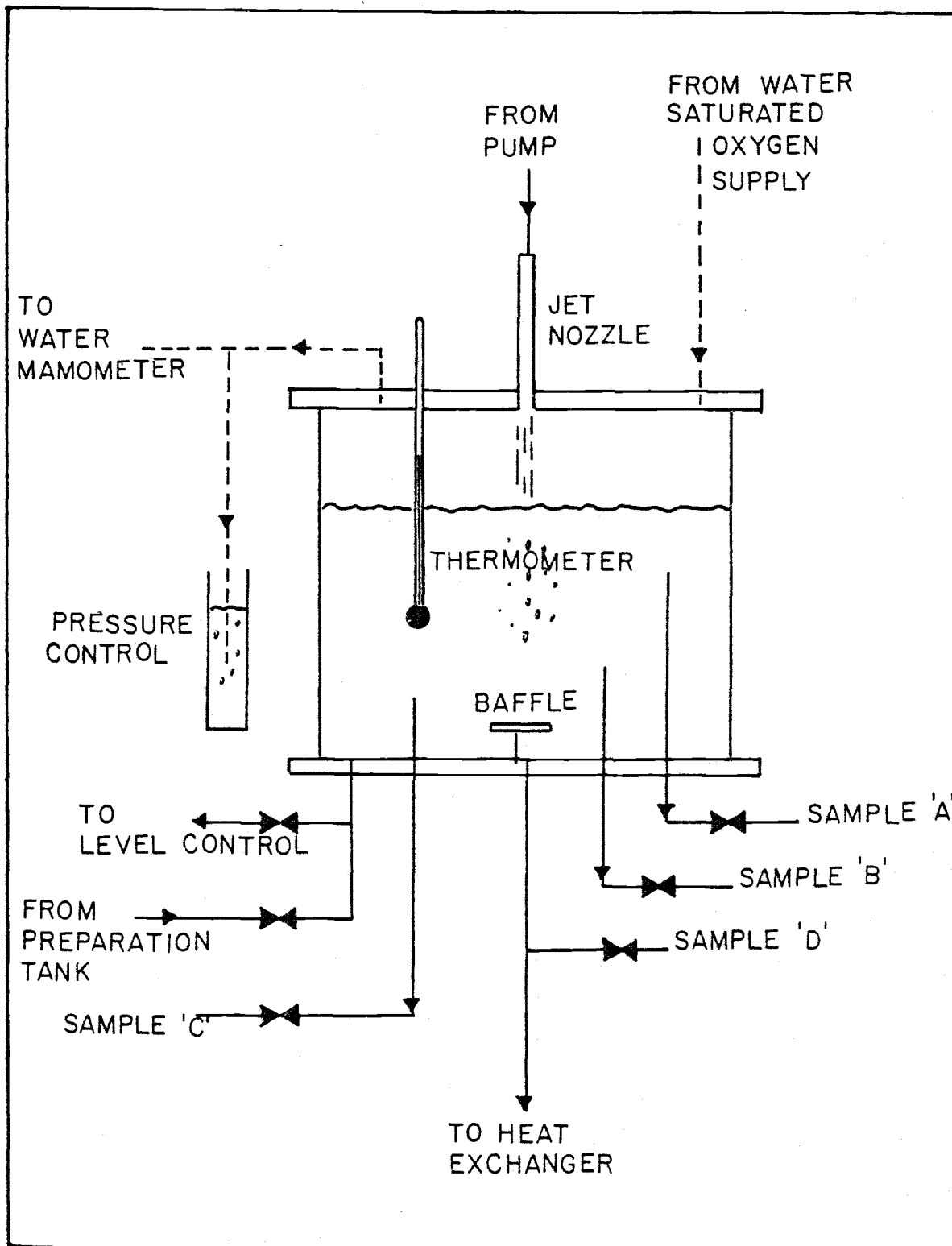


FIGURE 2. Details of absorption pool.

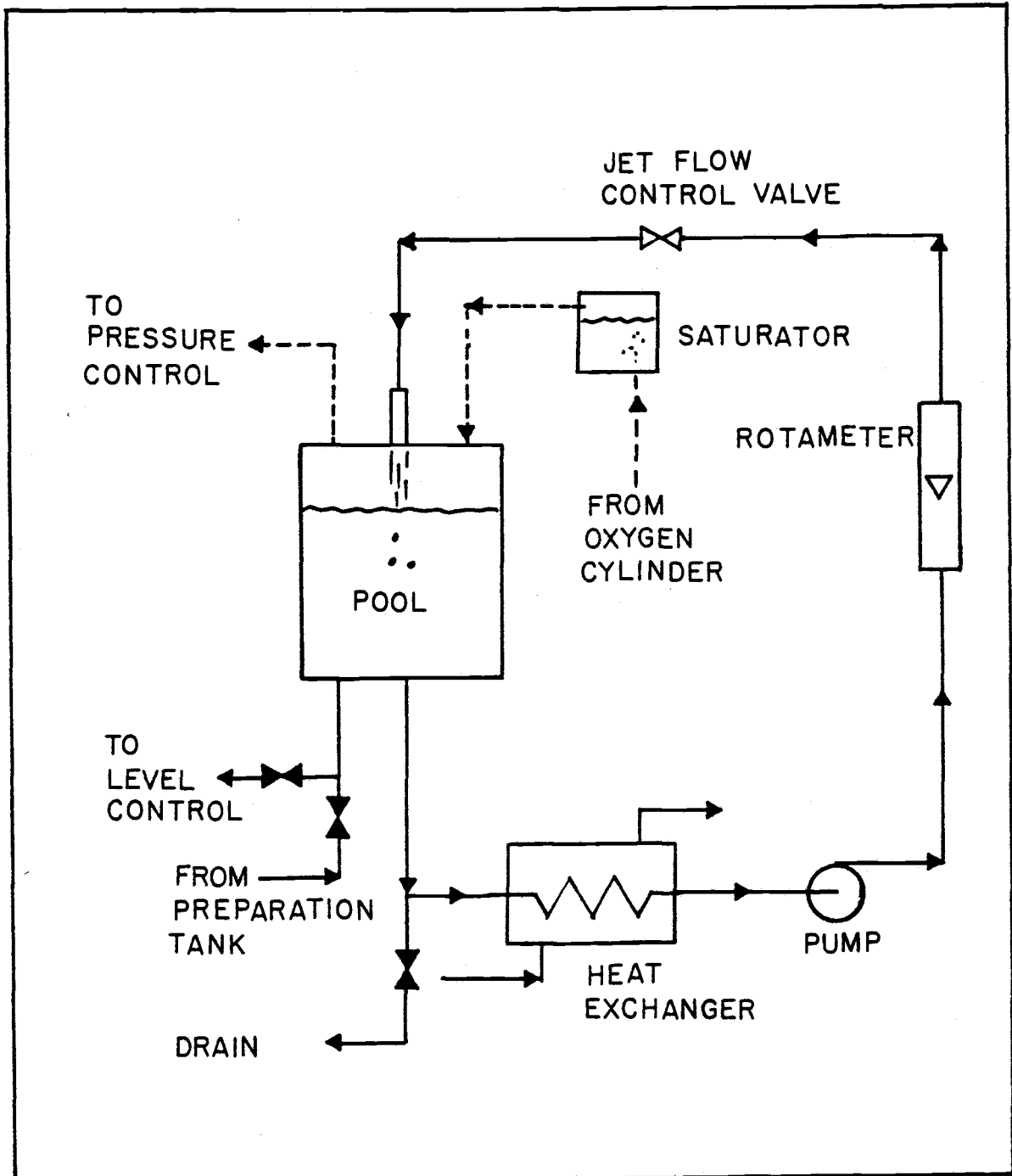


FIGURE 3. Schematic diagram of absorption pool.

The objective of this work was to obtain the oxygen concentration in the fluid as a function of the run time for various jet characteristics. The conditions of the runs were tabulated in Tables 2, 3, and 4.

TABLE 2. Experimental jet conditions with water as solvent.

Run Number	Jet	$N_{Re}$	$N_{We}$
001	M	18450	877
002	M	10419	280
003	S	16331	1648
004	S	10548	688
005	L	13060	349

TABLE 3. Experimental jet conditions with brine (1%) as solvent.

Run Number	Jet	$N_{Re}$	$N_{We}$
101	M	18305	880
102	M	16312	699
103	M	14321	538
104	M	10337	281
105	S	16202	1653
106	S	10465	690
107	L	12957	350

TABLE 4. Experimental jet conditions with brine (5%) as solvent.

Run Number	Jet	$N_{Re}$	$N_{We}$
501	M	17712	890
502	M	15783	707
503	M	13857	544
504	M	10002	284
505	S	15677	1672
506	S	10126	698
507	L	12537	354

Each run was separated into two portions. The first part was designed to study the combined surface and the bubble absorption rates. The second part was designed to measure only surface absorption, see Figure 4 for illustration. The result of these two investigations were used to determine the corresponding transfer factor, TF.

The major concern of this work was to measure the oxygen content in brine. Some methods of analysis were eliminated because new techniques were available. Two techniques were considered thoroughly prior to the choice of the oxygen electrode.

Gas chromatograph used by Hauxwell (8) was rejected for this work, because sodium chloride in the solution is non-volatile. Hence, sodium chloride would build up in the column and eventually ruin the column.

Oxygen electrode has been widely used; it gives rapid and accurate analysis oxygen in the fluid. The oxygen electrode can be equipped with a temperature compensation and the output signal can be registered on a recorder if desired.

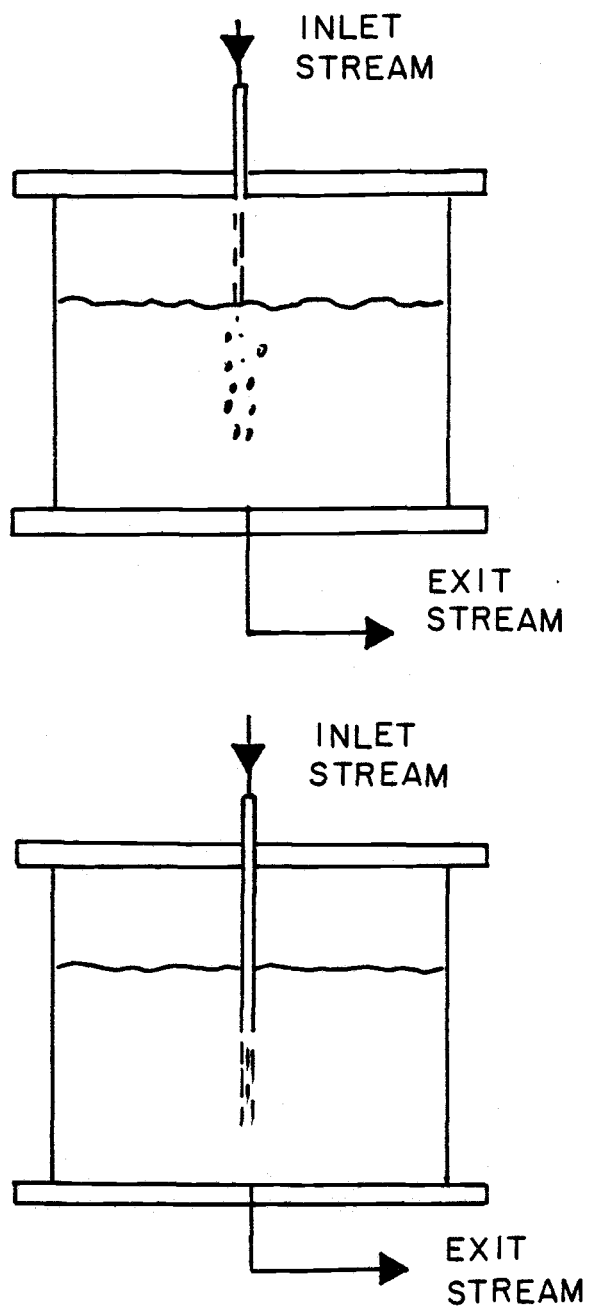


FIGURE 4. Study of total transfer factor (top) and surface transfer factor (bottom).

A flask, filled with distilled water, was saturated with air under atmospheric pressure. The air-saturated distilled-water was used to calibrate the oxygen meter. The pool samples were diluted with distilled water of known oxygen concentration. Then the oxygen concentration of the diluted samples was measured by the oxygen probe. The oxygen content in the pool samples was then calculated. The dilution process has two major beneficial aspects: (1) it reduces the salinity of the solution; (2) it makes the measurement of high oxygen content possible.

#### Procedure

The first step in every run was to calibrate the oxygen probe. The oxygen concentration of the distilled water used for dilution was measured before, during and after each run.

The enclosed cylinder was completely filled with water, and the proper flow rate and jet nozzle were set. The water in it was then drained while oxygen was fed simultaneously into the cylinder until the cylinder was totally filled with oxygen.

Brine was fed into the cylinder up to the operating level — 270 mm from the bottom. The temperature of the fluid was controlled at  $20 \pm 1^{\circ}\text{C}$ .

Excess oxygen was supplied continuously throughout the run, causing a steady flow rate. A higher pressure was maintained within the cylinder at 765 mm Hg with the submerged bubble device. This tended to prevent contamination inside the enclosed cylinder.

The jet nozzle was set at 90 mm above or below the pool surface for the appropriate runs. By using a constant jet length, one has eliminated one of the variables in this study. Van De Sande and Smith (22) indicates the absorption rate is also a function of jet length.

Samples were taken simultaneously after the run had started. Individual samples were contained in 16, 125 ml bottles. Four samples were taken during each time interval. The sample tubes were put at the very bottom of the bottles which were then filled to the top. The filled bottles were 'sealed' immediately with rubber stoppers. Sampling was continued over three more time periods. These samples were analyzed during and immediately after the run.

The 125 ml sample was transferred into a polyethelene bottle and diluted to 550 ml with distilled water of known oxygen content. A magnetic stirrer was used to give a perfectly mixed solution.

The probe acted like a stopper which sealed the solution from the environment. The oxygen concentrations of these diluted samples were recorded in ppm as indicated by the oxygen meter. The oxygen meter was provided with a scale between 0-20 ppm. In this work, a scale up to 40 ppm was required. Also, low salinity tends to give a more accurate analysis. Accordingly, a diluted sample was found desirable for these purposes.

Experimental results obtained were in the form of pool concentration as a function of both time and sample positions. Periodically, a sample of distilled water was analyzed to insure the oxygen content

remained constant. Air was bubbled into distilled water prior to use. The oxygen content of distilled water was very stable throughout the run.

Once the run was completed, the fluid was drained. The cylinder was partially filled and washed by water before beginning another run.

## DISCUSSION

The measurements of pool samples showed an uniform oxygen content throughout the fluid. Since the variations among the four samples were so small (less than 2% in most cases), the fluid was considered to be perfectly mixed in this work. Previous investigators, Hauxwell (8) and Van De Sande and Smith (22), also found good mixing in the pool.

Water was chosen as the first solvent. The results of the absorption of oxygen in water was compared with those of Hauxwell (8).

A special attempt was made to evaluate the change in TF by varying the jet length. A jet length of almost 4 times longer than the length employed by Huxwell (8) was used in this investigation. One has to bear in mind that other experimental conditions were very close between Hauxwell (8) and this work. A substantial change in TF was found. The differences in experimental conditions and correlations were tabulated and plotted in Figure 5.

Most of the experimental conditions were almost identical except the jet length. The deviation in TF is certainly caused by the tremendous change in jet length. By monitoring the jet length, one can observe a difference in bubbles' penetration depth (see Figure 6 for illustration).

When the jet nozzle is moved towards the pool surface, the bubbles' penetration depth increases. Also, gas bubbles are finer when jet length is shorter. That means, at shorter jet length, gas bubbles have longer duration in the solvent and larger interfacial surface area for same amount of entrained bubbles. Therefore, a

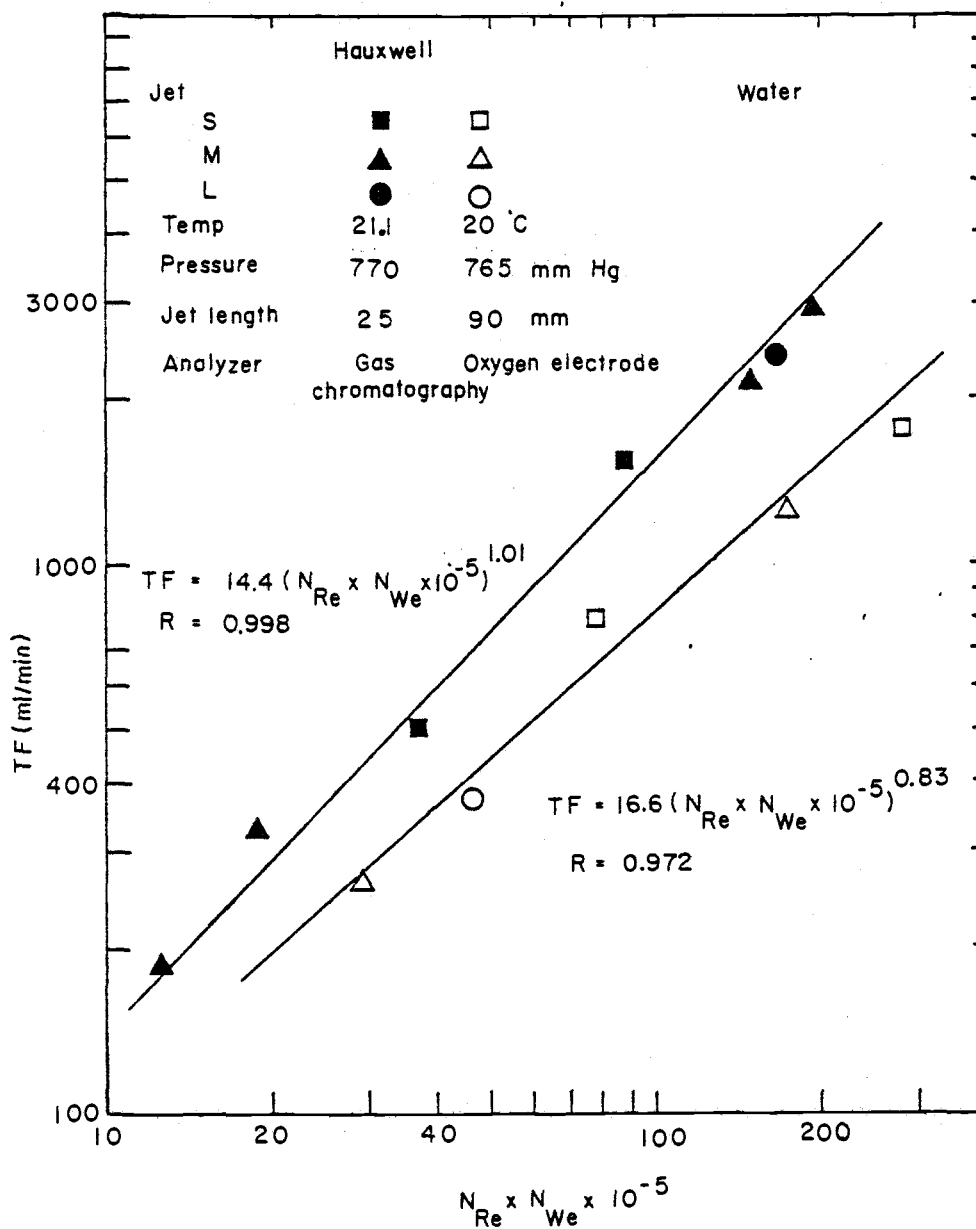


FIGURE 5. Comparison between Hauxwell (8) correlation and correlation of this work.

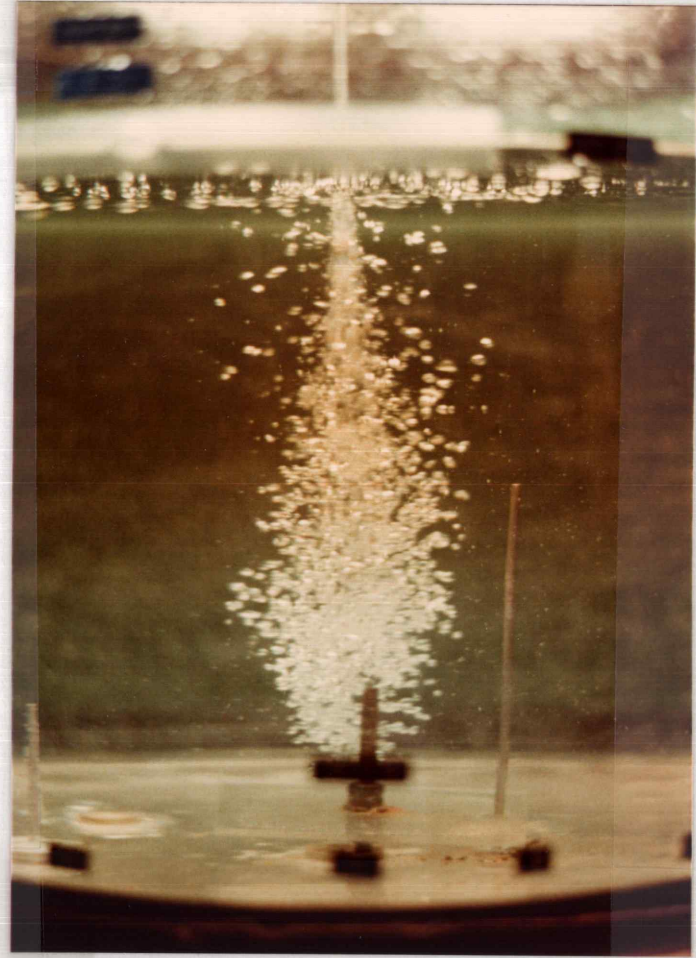
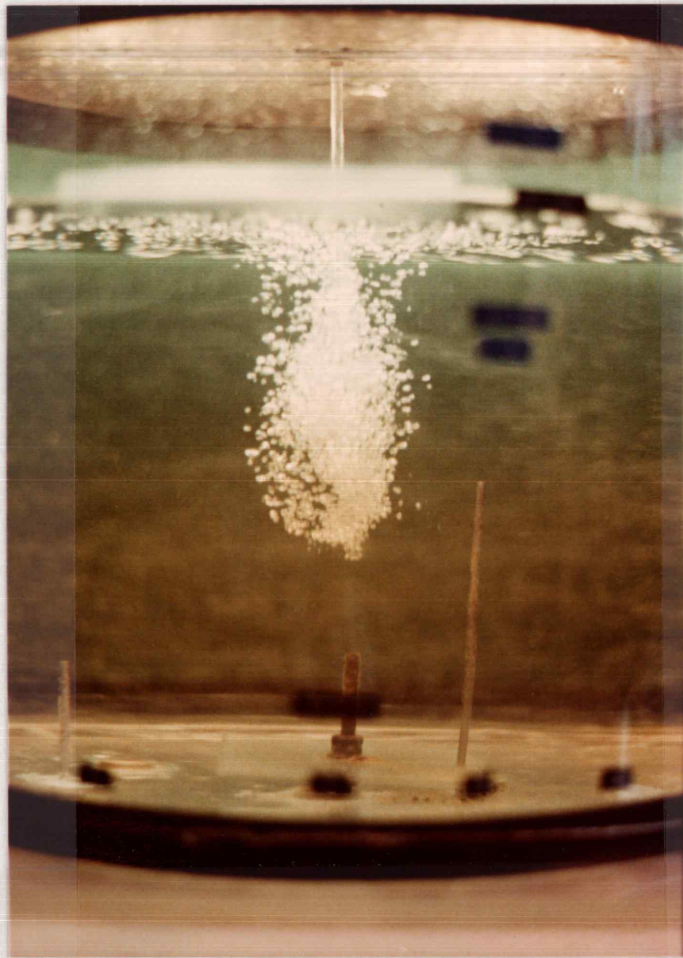


FIGURE 6. Bubble's penetration depth. Jet length = 90 mm (left). Jet length = 25 mm (right).

comparative increase in TF is expected.

However, a longer jet length entrains more bubbles than the shorter one. For the case of longer jet length, gas bubbles are more compact than those with shorter jet length. When bubbles are too close to each other, the interference among them might decrease the value of TF since there ought to be an increase in resistance. A maximum value for TF with same experimental conditions is suggested. However, no attempt has been made to complete a detail study because of inadequacy in the size of the cylinder.

Further study in this work was focused on the absorption in brine. A good correlation was found for both 1% and 5% brine (see Figure 7 and 9). The TF can be described by the product of  $N_{Re}$  and  $N_{We}$  which gives a very good relationship between them. This indicates the jet characteristic is very important in the mass transfer process. Of course, one has to bear in mind that the jet length was held constant throughout this work.

The temperature of the fluids was controlled at  $20 \pm 1^{\circ}\text{C}$ , pressure at 765 mm Hg., depth of the pool was 270 mm and the jet length was 90 mm.

A comparison of absorption for different sodium chloride content was plotted in Figure 10. An increase in TF for the corresponding increase in sodium chloride content was found. Also, from the plot, one can see the slopes for 1% solution and 5% solution are essentially identical. In other words, these two lines are almost parallel to each other.

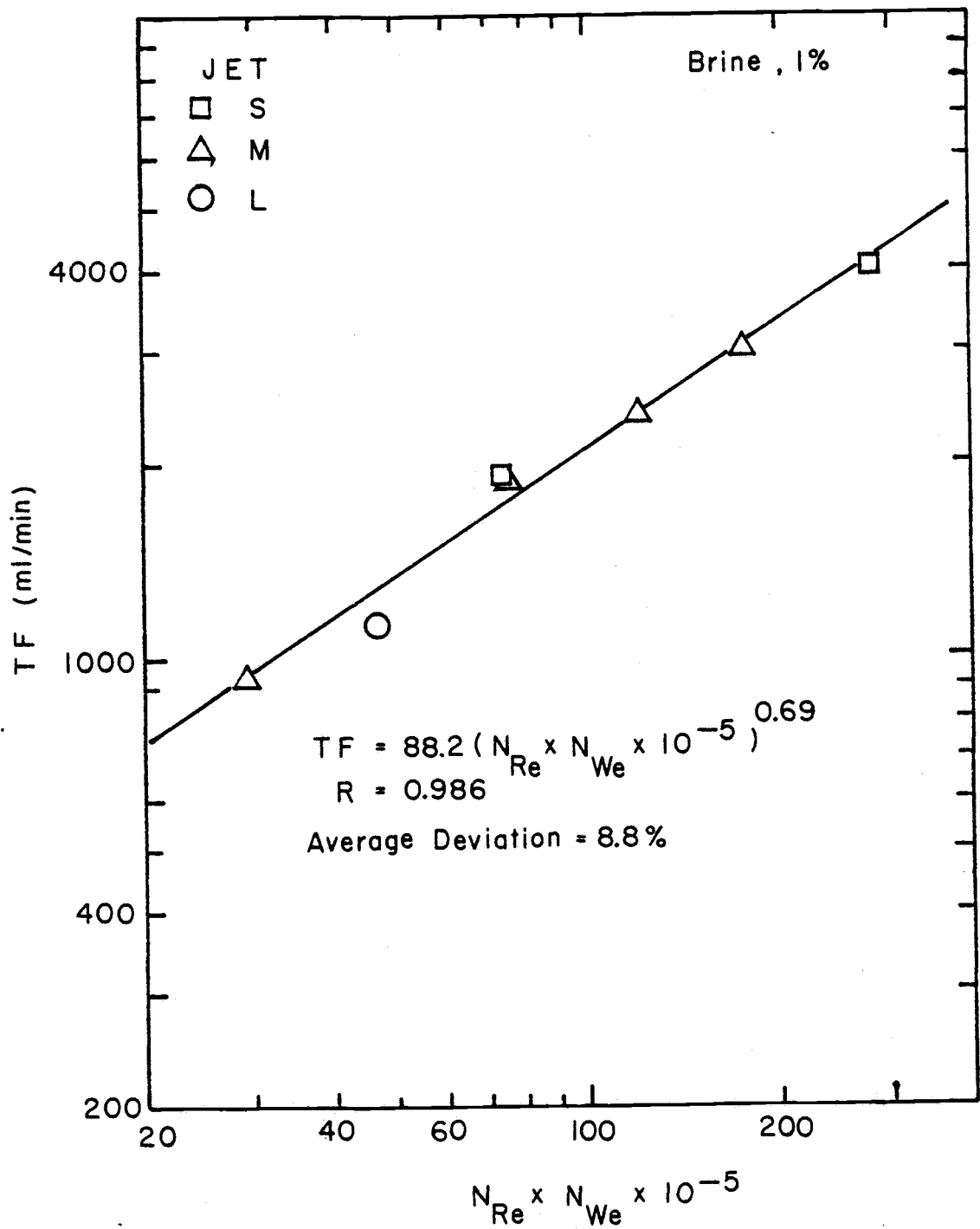


FIGURE 7. The TF for oxygen absorption in brine (1%).

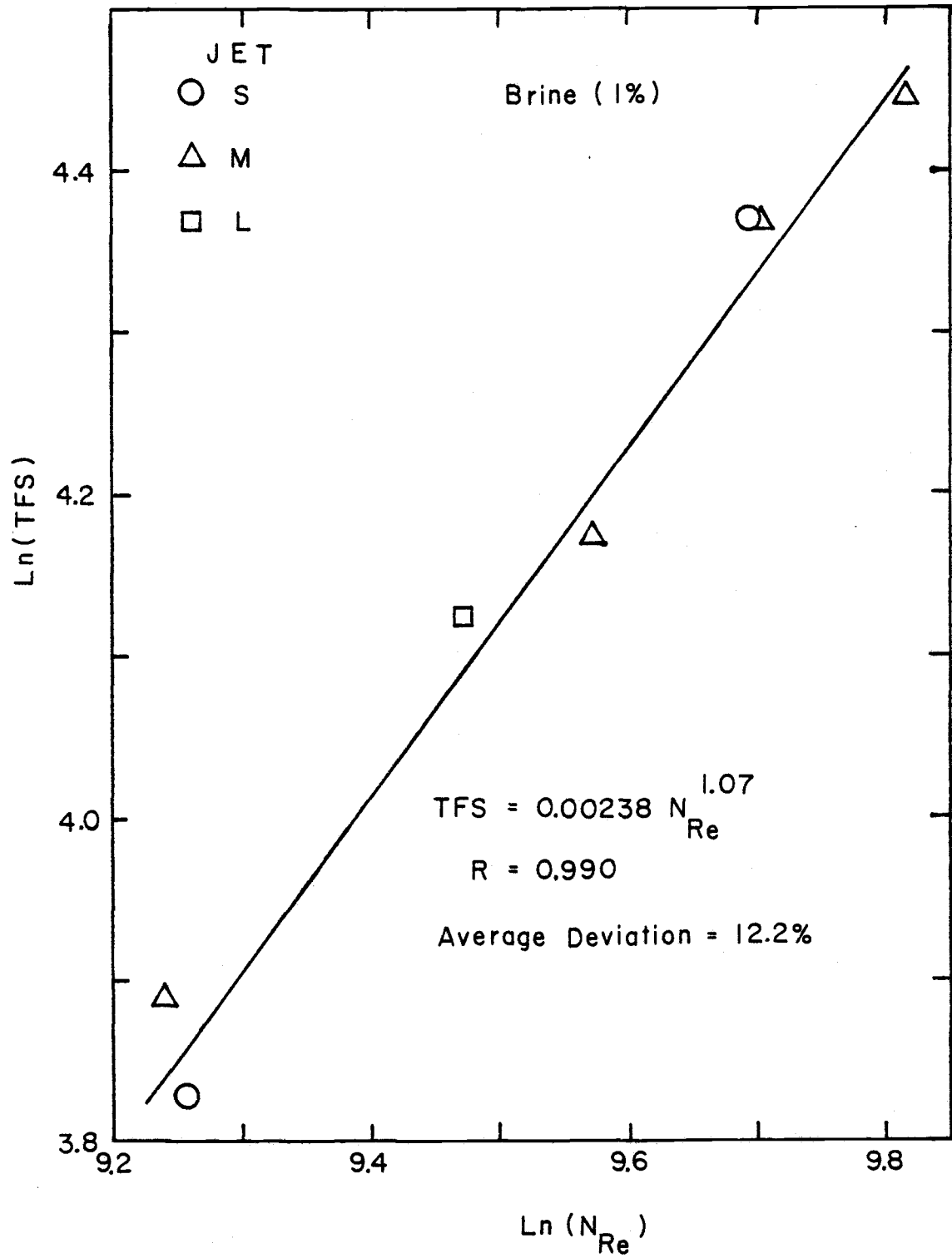


FIGURE 8. The TFS for oxygen absorption in brine (1%).

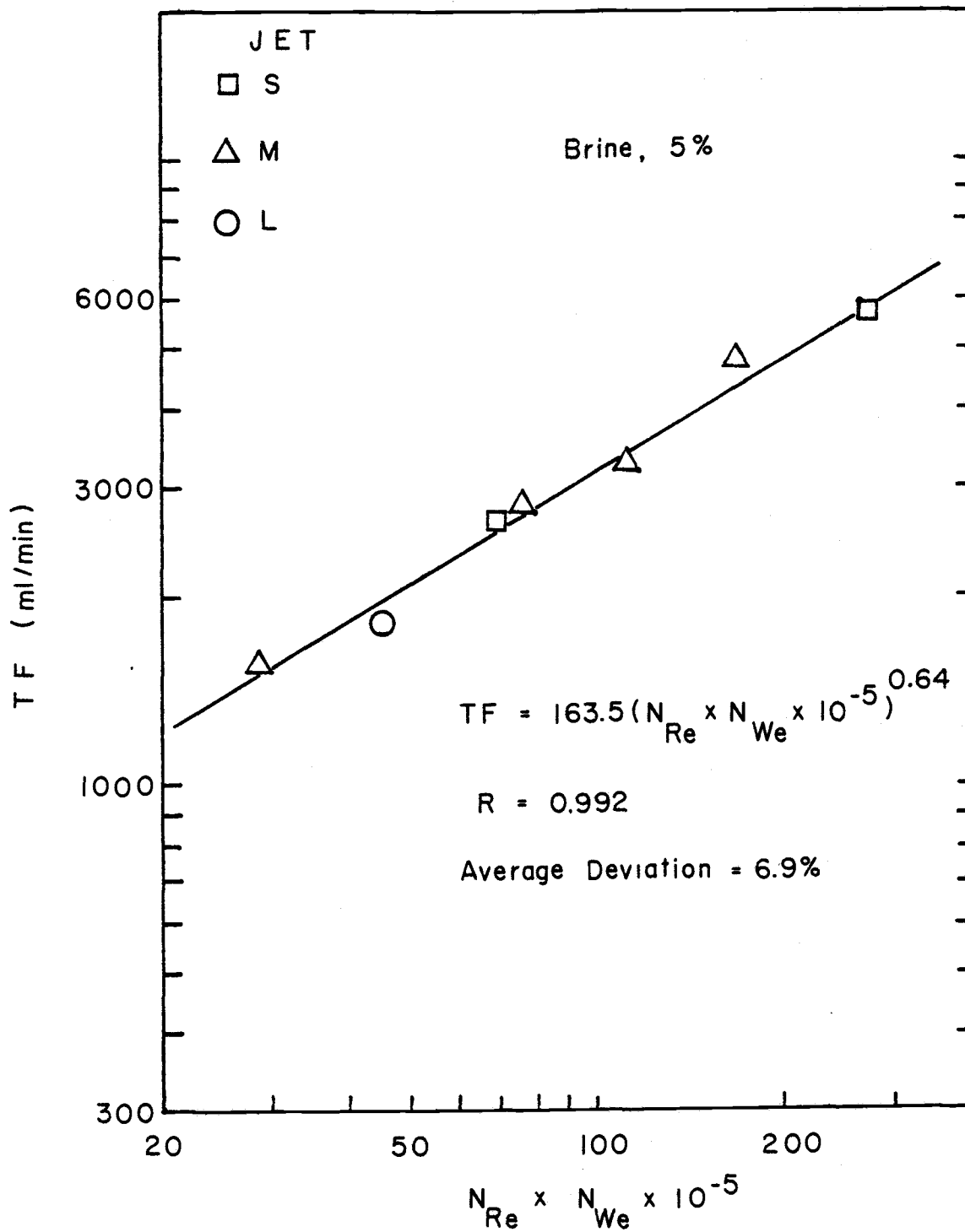


FIGURE 9. The TF for oxygen absorption in brine (5%).

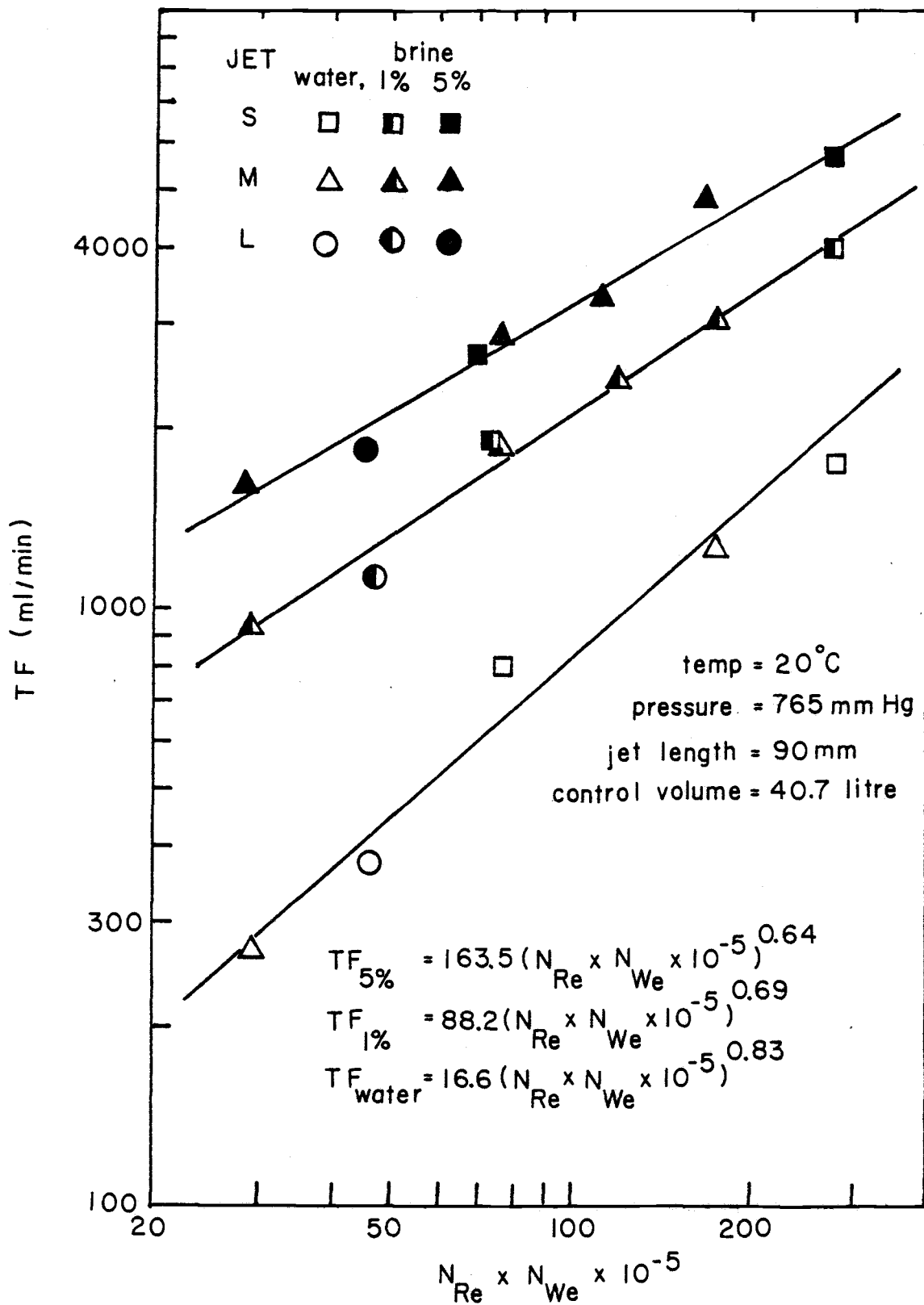


FIGURE 10. The TF for oxygen absorption in different solutions.

To understand this trend, one has to look into the intermolecular structure of water. A single isolated water molecule consists of two hydrogen atoms and one oxygen atom. The difference in electronegativity between the hydrogen and oxygen atoms forms a highly polar molecule. Hydrogen bondings are formed between water molecules because of the polarity of individual water molecules. Properties of water molecules are illustrated in Figure 11.

In liquid water, water molecules have great tendency to maintain the same type of structure as they have in the ice. Erdey-Grug (4) indicates that "even the most recent scientific works have not led to generally accepted results satisfactory in all respects." However, there is no doubt about the existence of water polymers in liquid water.

Water, a highly polar solvent, is capable of overcoming the interionic force of sodium chloride by forming new bonds between water molecules and ions. These ions destruct the ice-like structure of water and change the orientation of the dipole molecules of water. However, the actual structure of the ionic solution is very complex.

Horne (9) provided an explanation of the structure of ionic solution using  $\text{Na}^+$  as an example. The structure is illustrated in Figure 12. Taking  $\text{Na}^+$  ion as the center, it is surrounded by 4 primary hydrated water molecules. The second layer is surrounded by Frank-Wen cluster. The Frank-Wen cluster is water polymers existing in the solution as if there were no ions at all. There will be a lot of clusters within the ionic solution. Of course, this depends on the

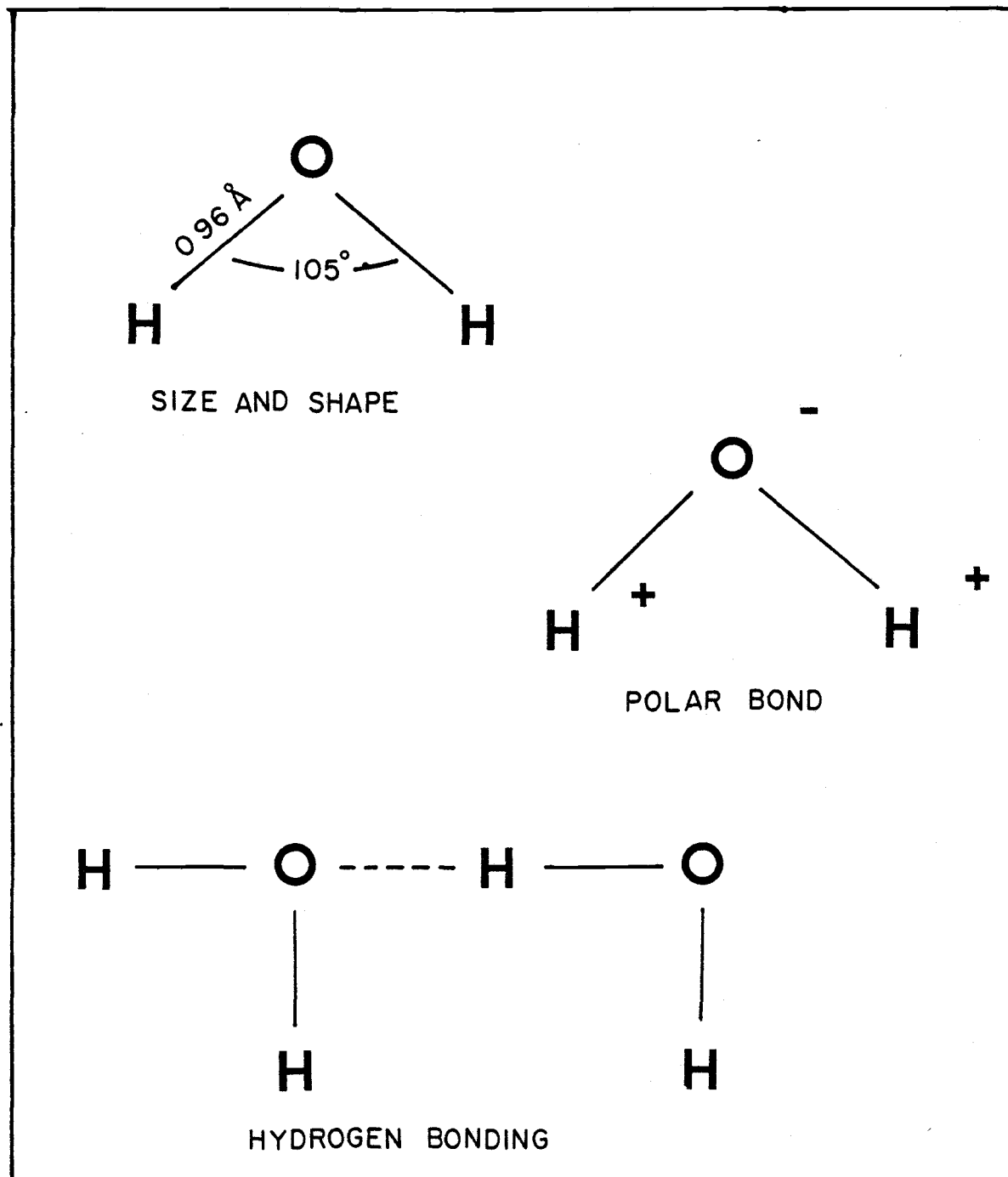


FIGURE 11. Structure of water molecule. From Morrison and Boyd (13).

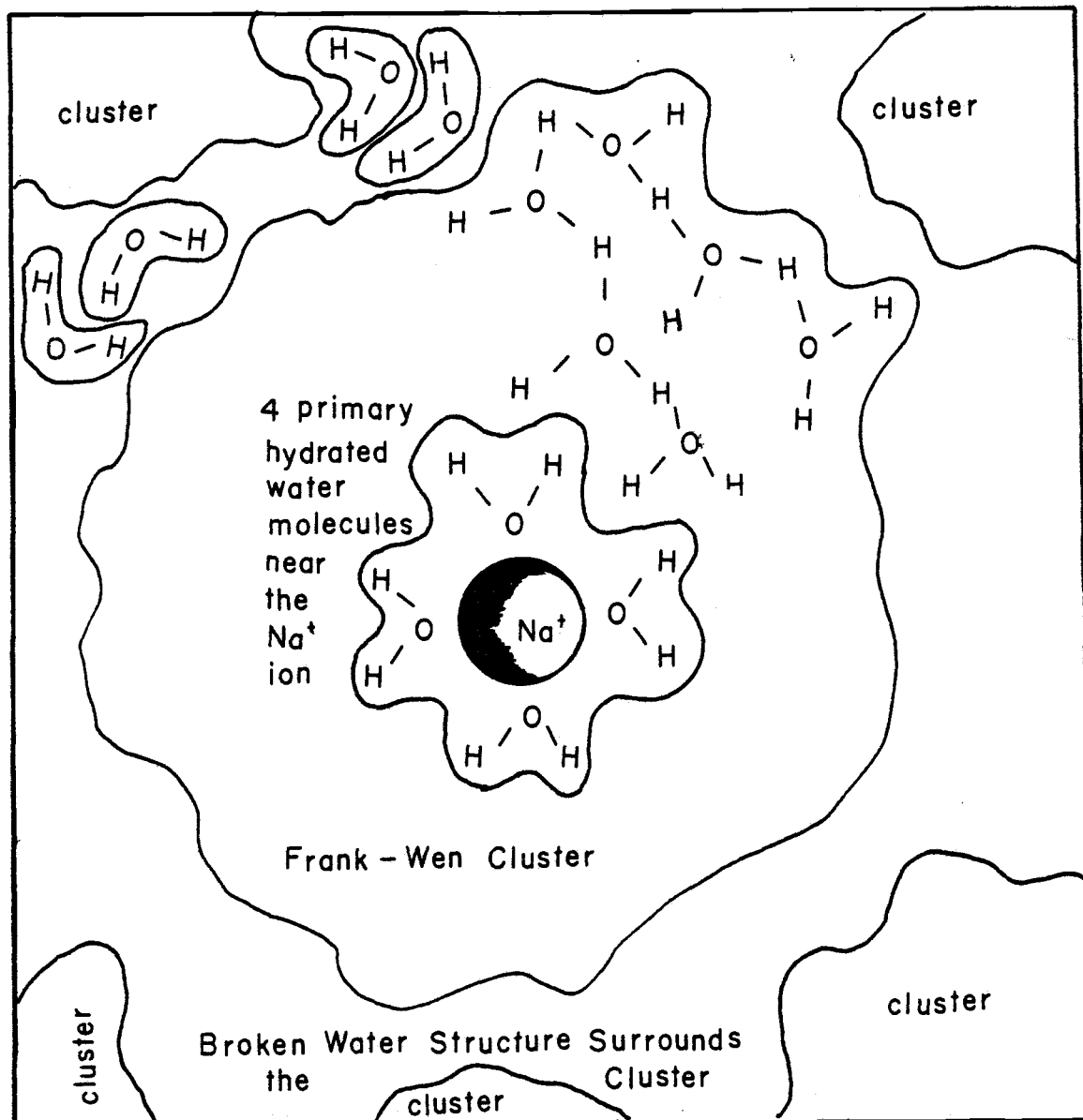


FIGURE 12. The structure of ionic solution. From Horne (9).

amount of ions. These clusters are separated by broken-water molecules—water monomers. This only explains the hydration process on  $\text{Na}^+$  ion. Horne (9) indicates that "the nature of the hydration spheres of anions is little understood." However, one can still conclude that there are more water monomers in ionic solution than in liquid water.

In order to overcome the strong interionic force of sodium chloride crystals, a large amount of hydrogen bondings has to be destructed in order to supply enough energy for hydration. Therefore, a large quantity of 'free' water monomers will be formed. The increase in water monomers allows the water molecules to move more freely. Erdey-Gruz (4) states that "the mobility of water molecules is increased by destroying the lattice-like structure of water."

An increase in the mobility of water molecules should give a corresponding increase in the TF, since the probability of solute gas in contact with more solvent molecules is increased.

As observed in the experimental work, there is a substantial increase in the amount of minute bubbles (smaller than 0.5 mm in diameter) as the concentration of sodium chloride increases. In the case of water as the solvent, there was practically no tiny bubbles suspended in the fluid. Fine bubbles could be seen throughout the brine pool. They were evenly distributed throughout the fluid. The small bubbles remained suspended in the fluid after the pump has been turned off for about a couple of minutes. There is no doubt about the tremendous increase in the interfacial area between solute gas and solvent. This, in return, increased the TF.

Pictures were taken of the entrainment process for different solvents. One has to keep in mind these pictures (see Figure 13) were taken for the same jet size, same volumetric flow rate, same shutter speed (1/250 sec) and same aperture. The difference between the entrainment process in water and in brine is very obvious. The bubbles were confined to one zone when water was the solvent. In the case of brine, bubbles were more dispelled. Basically, it can be divided into three regions; (1) the primary zone contains all the big bubbles, (2) the secondary zone contains bubbles of medium sizes, (3) the tertiary zone contains all the fine bubbles in it. This phenomenon suggested that oxygen has a higher probability for forming smaller bubbles in brine.

The work done in the entrainment process is purely by the kinetic energy of the jet. There is no other source of work input. The size of bubble formed depends on work input, turbulence of the fluid, as well as the hydrodynamic properties of the fluid. With this reasoning, the hydrodynamic situation and the turbulence of brine is more favorable in the formation of tiny bubbles. The values of TF increase substantially when the concentration of sodium chloride in the solution increases. Holding all other factors constant, the values of TF is directly related to the turbulence and hydrodynamic situation of the fluid.

To understand the rate of absorption caused by the tremendous change in the TF, calculations were performed using Equations (8) and (9).

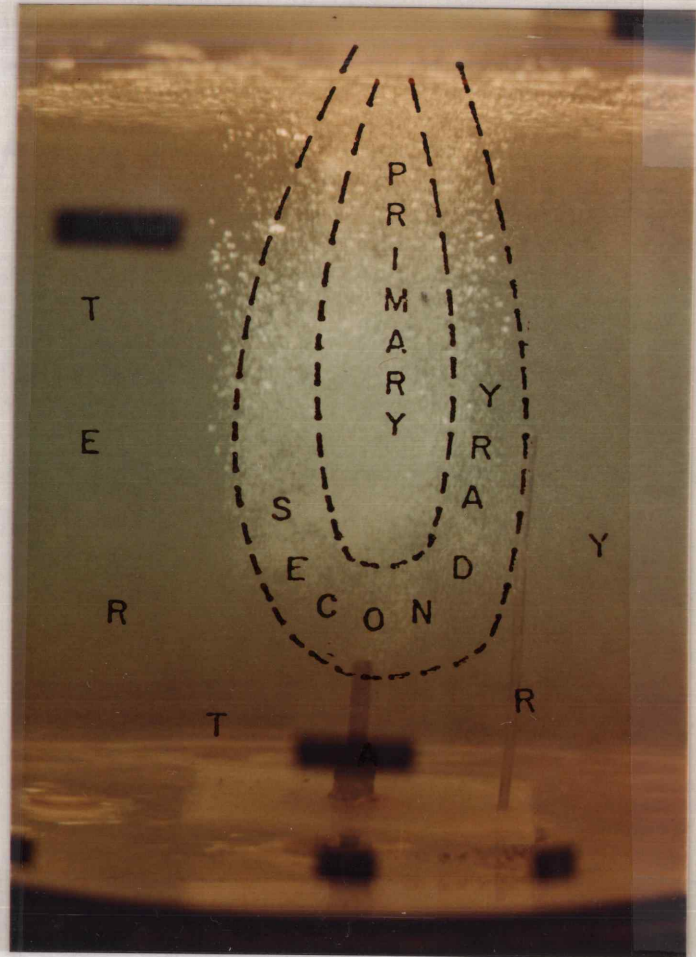
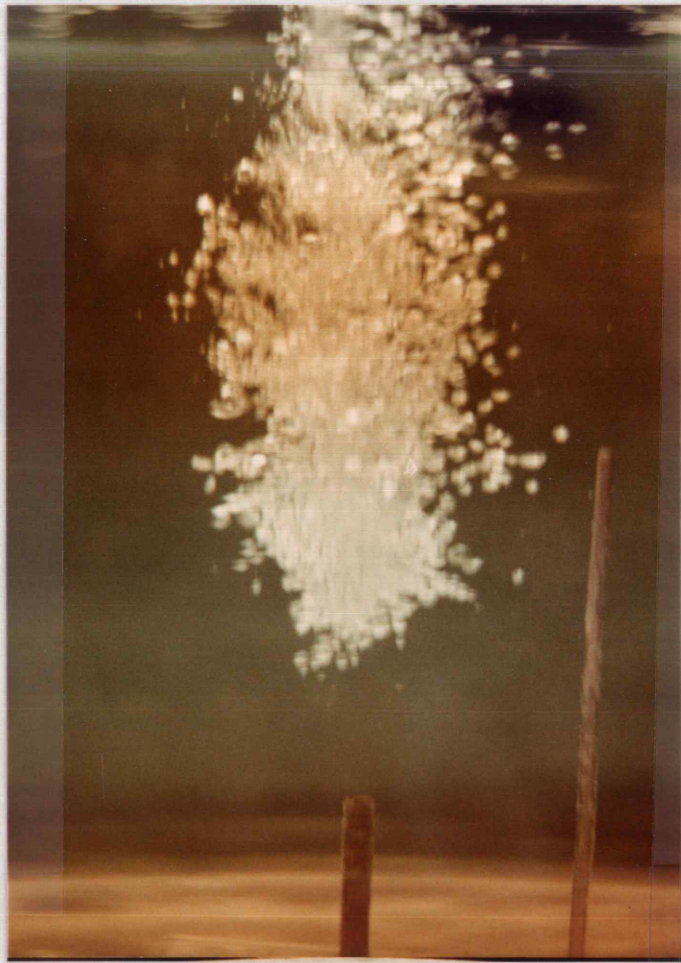


FIGURE 13. Oxygen bubbles in different solvents; water (left), Brine (5%) (right).

$$W_B = TF (C^* - C_L) \quad (18)$$

For simplicity, assume  $C_L = 0$ . A set of runs with the same volumetric flow rates were used in the calculations. The values were tabulated in Table 5 and plotted on Figure 14.

TABLE 5. Comparison of the rate of absorption.

Run Number	TF ml/min	$C^*$ mg/l	$W_B$ mg/sec
001	1202	9.20	0.18
½01	2354	8.89	0.35
101	3001	8.61	0.43
201	3339	8.12	0.45
501	4710	5.22	0.41

When the concentration of sodium chloride in the solution increases, the solubility of oxygen decreases. However, the TF increases. Since the rate of absorption is a function of solubility of oxygen and TF, there exists a maximum value for the rate of absorption. Actually, one can simply look at Equation (18) and sketch the shape of curve for the rate of absorption vs. the concentration of sodium chloride without any difficulty.

Some detail observations were made during the runs. When water is used as the solvent, there are a lot of bubbles (about 1 mm in diameter) attached to the wall of the cylinder (see Figure 15). However, the amount of bubbles attached to the cylinder wall decreases very substantially when aqueous sodium chloride solution is used as

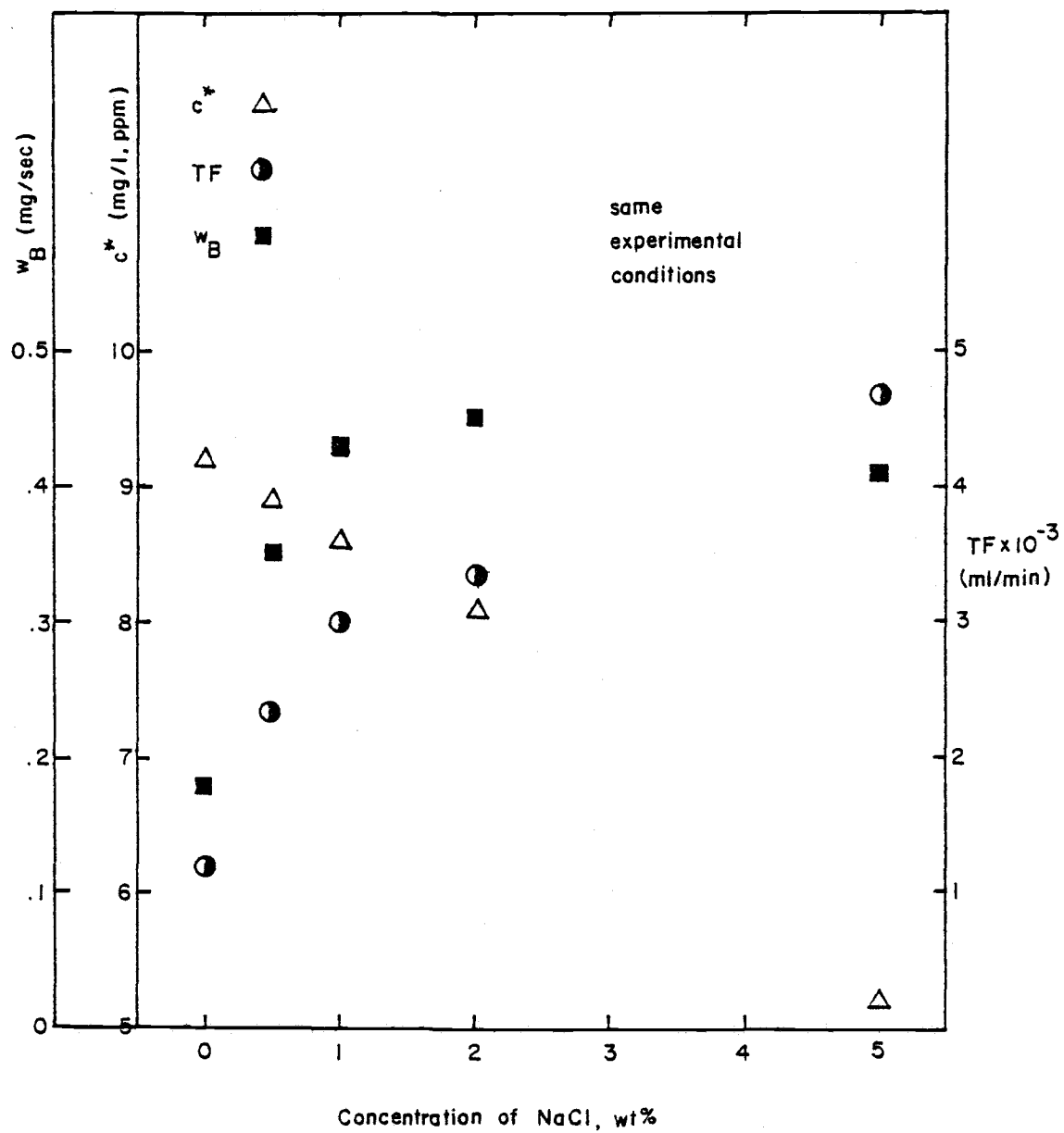


FIGURE 14. Comparison of rate of absorption.

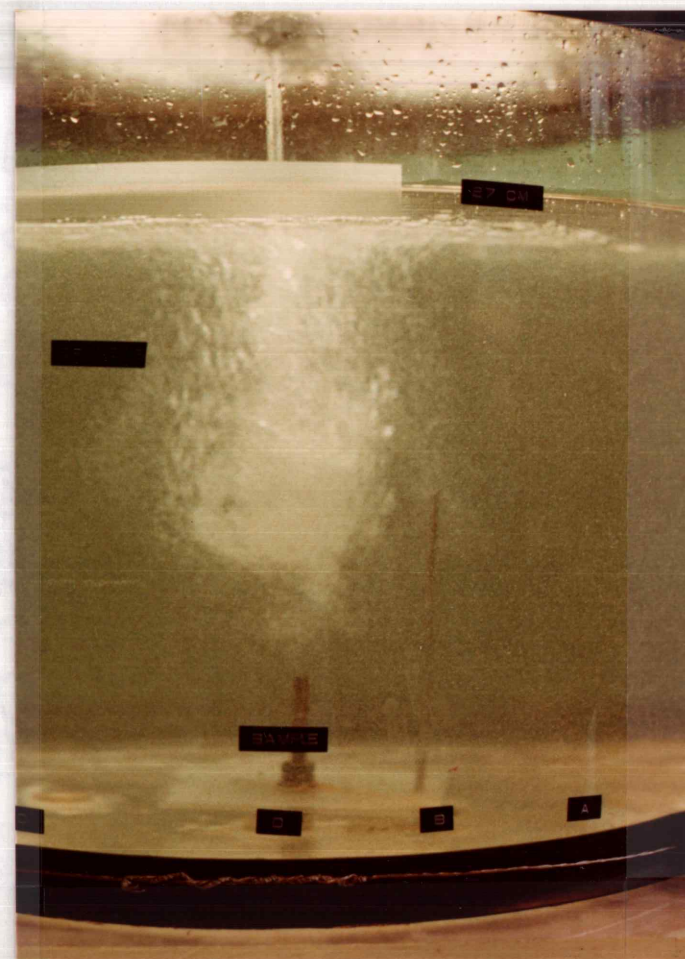
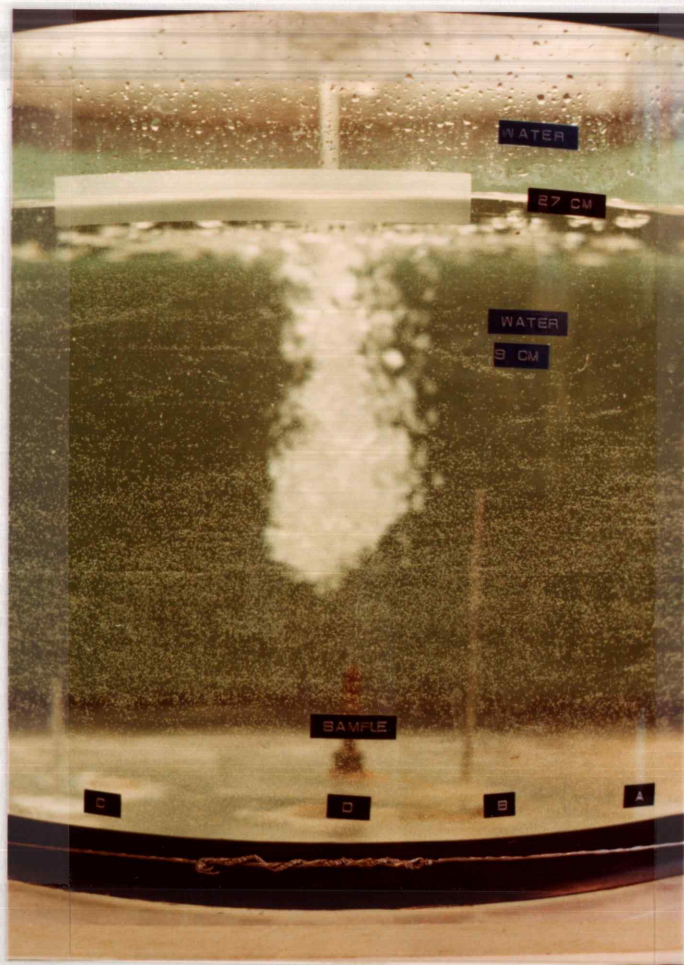


FIGURE 15. Amount of bubbles attached to the cylinder wall in different solvents. Water (left), Brine, 5% (right).

the solvent. There is practically no gas bubble attached to the wall when 10% sodium chloride solution is used as the solvent. This suggested that oxygen bubbles are more 'comfortable' in aqueous sodium chloride solution than in water. Hence, the hydrodynamic properties of the solvent plays an important role in mass transfer process.

Table salt was used in several runs. The impurities in table salt gave a very 'cloudy' solution. For identical experimental conditions, the TF in table salt solution was significantly lower than the TF in sodium chloride (99.5% pure) solution. The impurities in table salt tends to increase the interfacial resistance. That is the coefficient of mass transfer will decrease. Since the TF is a function of coefficient of mass transfer, the values of TF is directly proportional to the coefficient of mass transfer. Hence, the impurities in the solution can not be ignored.

The values of TF was compared with the corresponding values of TFS. One can see that the effect of TFS is very small throughout the range of investigation in this work (see Appendix III, Table III-61). In this work, the change caused by TFS was less than 5%.

Finally, there was no attempt to correlate the relationship of TF with respect to the concentration of sodium chloride in the solution. The change in hydrodynamic situation, the impurities and the jet length has a direct impact on the actual mass transfer process. A correlation would not be meaningful unless these variations could be compensated for in the correlation.

## CONCLUSION

The conclusions of the study of oxygen absorption as a result of a plunging jet are:

1. A plunging jet creates enough turbulence in the fluid to maintain a perfectly mixed solution at all times. The solution will be saturated with oxygen in every short period of time as the result of a plunging jet.

2. The variation in jet length has a direct impact in TF. The TF is directly related to bubbles' penetration depth, the size of entrained bubbles, and the closeness of the bubbles. These factors are all interrelated. By monitoring the jet length and keeping all other experimental conditions identical, the curve of TF vs jet length could give a maximum value.

3. In all the studies, the TF is found to be proportional to the product of jet stream  $N_{Re}$  and  $N_{We}$ . That shows the same type of approach can be used for various solution as long as there is only one variable at a time.

4. The TF is found to be directly proportional to the concentration of sodium chloride in the solution. The hydrodynamic situation of the ionic solution increases the mobility of water molecules. The tremendous amount of tiny bubbles formed in brine increases the interfacial area between solvent and solute gas. Accordingly, there is a substantial increase in TF. On the other hand, the solubility of oxygen is inversely proportional to the concentration of sodium chloride in the solution. Hence, there exists a maximum value for

the rate of absorption.

5. Impurities in the solution increases the interfacial resistance between the gas and liquid phase. This has a direct impact in the mass transfer process. The change in TF is very significant.

In brief, the TF is a function of  $N_{Re}$  and  $N_{We}$  of the jet stream. The jet length should be the same throughout the investigation and the impurities in the solution should 'hold constant'.

## RECOMMENDATIONS

1. A wide range of variation of liquid density, viscosity and surface tension are of immediate interest. These variations caused by solute other than sodium chloride is highly recommended.

2. A system with multi-jet nozzles is recommended for further study.

3. A solute gas which has chemical reaction with the solvent is of immediate interest. This chemical reaction will probably change the liquid properties considerably.

4. A extensive study of the dependency of TF on the jet length is highly recommended.

5. A thorough study of the influence of impurities might give a promising way in the determiation of TF.

## NOMENCLATURE

<u>Symbol</u>	<u>Significance</u>
A	- area
C	- concentration of solute
D	- diameter
$g_c$	- force-mass conversion factor
K	- overall mass transfer coefficient
k	- mass transfer coefficient
L	- length
$N_{Re}$	- Reynolds number ( $D_J v_J \rho / \mu$ )
$N_{We}$	- Weber number ( $D_J v_J^2 \rho / \sigma g_c$ )
Q	- volumetric flow rate
R	- coefficient of correlation
t	- time
TF	- transfer factor (Equation (9))
TFS	- surface transfer factor (Equation (10))
TTF	- total transfer factor (Equation (11))
V	- pool volume
v	- velocity
W	- rate of absorption
z	- dimensionless group (Equation (15))

Greek

$\mu$	- viscosity
$\rho$	- density
$\sigma$	- surface tension

<u>Symbol</u>	<u>Significance</u>
---------------	---------------------

<u>Subscript</u>	
------------------	--

B	- bubble
E	- exit stream
I	- inlet stream
i	- interface
J	- jet
j	- jth
L	- liquid
o	- initial condition
Re	- Reynolds
S	- surface
We	- Weber

<u>Superscript</u>	
--------------------	--

*	- equilibrium value
+	- dimensionless value

## BIBLIOGRAPHY

1. Bird, R. B., W. E. Stewart and E. N. Lightfoot. 1960. Transport phenomena. New York, Wiley, 780 p.
2. Carpenter, J. H. 1966. New measurements of oxygen solubility in pure and natural water. *J. Limnology and Oceanograph.* 11:264-277.
3. Degn, H., I. Balslev and R. Brook (ed.). 1976. Measurement of oxygen. New York, Elsevier Scientific Publishing Co., 276 p.
4. Erdey-Gruz, T. 1974. Transport phenomena in aqueous solutions. New York, Wiley, 512 p.
5. Franks, F. (ed.). 1973. Water. V.1 and V.3. New York, Plenum Press, n. p.
6. Gal-Or, B., J. P. Hauck and H. E. Hoelscher. 1967. A transient response method for a simple evaluation of mass transfer in liquids and dispersions. *International Journal of Heat and Mass Transfer.* 10:1559-1570.
7. Gurney, R. W. 1953. Ionic processes in solution. New York, McGraw-Hill, 275 p.
8. Hauxwell, G. D. 1972. Pool absorption of gas entrained by plunging liquid jet. PhD thesis. Corvallis, Oregon State University, 187 numb. leaves.
9. Horne, R. A. (ed.). 1972. Water and aqueous solutions. New York, Wiley, 837 p.
10. Jackson, M. L. 1964. Aeration in Bernoulli types of devices. *AIChE Journal.* 10:836-842.
11. Lange, N. A. (ed.). 1956. Handbook of chemistry. 9th ed. Sandusky, Handbook Publishers, Inc. 1969 p.
12. Moore, W. J. 1972. Physical chemistry. 4th ed. Englewood Cliffs, Prentice-Hall, 977 p.
13. Morrison, R. T. and R. N. Boyd. 1973. Organic chemistry. 3rd. ed. Boston, Allyn and Bacon, 1258 p.
14. Neter, J. and W. Wasserman. 1974. Applied linear statistical models. Homewood, Richard D. Irwin Inc., 842 p.

15. Perry, R. H. (ed.). 1973. Chemical engineer's handbook. 5th ed. New York, McGraw-Hill, n. p.
16. Rand, M. C. (ed.). 1976. Standard methods for the examination of water and wastewater. 14 ed. Washington, D.C., American Public Health Association, 1193 p.
17. Sherwood, T. K., R. L. Pigford and C. E. Wicks. 1975. Mass Transfer. New York, McGraw-Hill, 677 p.
18. Smigelschi, O., and G. Dan Suciu. 1977. Carbon dioxide absorption by turbulent plunging jets of water. Chemical Engineering Science. 32:889-897.
19. Spiegel, M. R. 1961. Theory and problems of statistics. New York, McGraw-Hill, 359 p.
20. Swiggett, G. E. 1969. Gas absorption by entrainment from a plunging liquid jet. PhD thesis. Corvallis, Oregon State University. 103 numb. leaves.
21. Tajar, J. G. and I. F. Miller. 1972. The permeation of carbon dioxide, oxygen, and nitrogen through weakly basic polymer membranes. AIChE Journal. 18:78-83.
22. Van de Sande, E. and J. M. Smith. 1975. Mass transfer from plunging water jets. The Chemical Engineering Journal. 10:225-233.
23. Weast, R. C. (ed.). 1972. Handbook of chemistry and physics. 53rd ed. Cleveland, The Chemical Rubber Co., n. p.
24. Welty, J. R., C. E. Wicks and R. E. Wilson. 1976. Fundamentals of momentum, heat and mass transfer. 2nd ed. New York, Wiley, 789 p.

## APPENDICES

## APPENDIX I

Experimental Code

Each run was coded as follows

Run Number: dbb

Run Conditions: a - d - xxxxx - yyyy - c

a = jet designation, i.e., S, M, L

bb = reference number

c = run purposes:

S = surface absorption

B = bubble and surface absorption

d = concentration of sodium chloride in wt%

xxxxx = jet stream  $N_{Re}$

yyyy = jet stream  $N_{We}$

## APPENDIX II

Equipment and Material Specification

TABLE II-1. Centrifugal pump

Mfgr.	Eastern
Model	E-7
Motor size	1/15 HP

TABLE II-2. Oxygen meter

Mfgr	Yellow Springs Instrument Co.
Model	54A

TABLE II-3. Material specification

Oxygen	Medical USP Grade - 99.59% pure
Sodium chloride	Reagent Grade - 99.5% pure

## APPENDIX III

Experimental DataTABLE III-1. Physical properties of water and brine at 20°C.  
From Weast (23).

NaCl (wt %)	Density (gm/ml)	Kinematic viscosity (centistokes)	Surface tension (dynes/cm)
0	0.998	1.007	72.75
0.5	1.0018	1.009	72.835*
0.58	--	--	72.92
1.0	1.0053	1.015	73.07*
2.0	1.0125	1.023	73.44*
2.84	--	--	73.75
5.0	1.034	1.049	74.28*
5.43	--	--	74.39
10	1.0707	1.115	--
10.46	--	--	76.05

\* By linear extrapolation

TABLE III-2. Solubility of oxygen in water exposed to water saturated air.\* From Rand (16).

Temperature (°C)	Chloride concentration in water mg/l				
	0	5000	10000	15000	20000
	Dissolved oxygen mg/l				
18	9.5	9.1	8.6	8.2	7.7
19	9.4	8.9	8.5	8.0	7.6
20	9.2	8.7	8.3	7.9	7.4
21	9.0	8.6	8.1	7.7	7.3
22	8.8	8.4	8.0	7.6	7.1

\* Assuming dry air contains 20.9% oxygen.

Linear extrapolation at 20°C

3064	8.89360
6127	8.60984
12254	8.11968

TABLE III-3. Measurement of oxygen saturated 5% brine.

Dissolved oxygen ppm		
Diluted * Sample	Make-up Water	Actual Sample
13.05	8.65	5.05745
13.15	8.65	5.14350
13.25	8.68	5.20815
13.42	8.68	5.35443
13.40	8.70	5.32295
13.20	8.70	5.18653
13.40	8.75	5.28727
Average =		5.22290
s =		0.10541
s/Average =		0.02

\* 125 ml of oxygen saturated sample was diluted to 550 ml.

TABLE III-4. Measurements of oxygen content of diluted samples for run M-0-18450-877-B.

Sample positions	Time (min.)			
	0	5	10	15
A	9.10	10.40	11.35	11.98 ppm
B	9.10	10.42	11.44	12.00
C	9.14	10.35	11.40	11.84
D	9.02	10.20	11.20	11.82

Oxygen content of make-up water: 8.65 ppm

TABLE III-5. Measurements of oxygen content of diluted samples for run M-0-10419-280-B.

Sample positions	Time (min.)			
	0	5	10	15
A	9.38	9.55	9.9	10.15 ppm
B	9.40	9.65	9.98	10.20
C	9.31	9.58	9.90	10.10
D	9.34	9.65	9.99	10.20

Oxygen content of make-up water: 8.65 ppm

TABLE III-6. Measurements of oxygen content of diluted samples for run S-0-16331-1648-B.

Sample positions	Time (min.)			
	0	5	10	15
A	9.15	10.75	11.75	12.42 ppm
B	9.22	10.85	11.85	12.45
C	9.20	10.65	11.78	12.65
D	9.15	10.62	11.82	12.60

Oxygen content of make-up water: 8.67 ppm

TABLE III-7. Measurements of oxygen content of diluted samples for run S-0-10548-688-B.

Sample positions	Time (min.)			
	0	5	10	15
A	8.98	9.82	10.50	11.02 ppm
B	8.86	9.70	10.61	10.95
C	8.94	9.70	10.44	10.95
D	8.98	9.6	10.40	10.80

Oxygen content of make-up water: 8.21 ppm

TABLE III-8. Measurements of oxygen content of diluted samples for run L-0-13060-349-B.

Sample positions	Time (min.)			
	0	5	10	15
A	8.98	9.42	9.78	10.30 ppm
B	9.00	9.35	9.80	10.15
C	9.00	9.38	9.70	10.04
D	8.98	9.40	9.78	10.15

Oxygen content of make-up water: 8.47 ppm

TABLE III-9. Measurements of oxygen content of diluted samples for run M-1-18305-880-B.

Sample positions	Time (min.)			
	0	5	10	15
A	8.60	11.20	12.50	12.90 ppm
B	8.50	11.20	12.60	12.80
C	8.40	10.82	12.60	13.30
D	8.30	10.80	11.80	13.20

Oxygen content of make-up water: 7.6 ppm

TABLE III-10. Measurements of oxygen content of diluted samples for run M-1-16312-699-B.

Sample positions	Time (min.)			
	0	5	10	15
A	9.00	11.20	11.90	13.10 ppm
B	9.10	11.30	12.40	13.00
C	9.00	10.80	11.80	12.60
D	9.00	10.70	12.20	12.70

Oxygen content of make-up water: 8.0 ppm

TABLE III-11. Measurements of oxygen content of diluted samples for run M-1-14321-538-B.

Sample positions	Time (min.)			
	0	5	10	15
A	8.60	10.40	11.20	12.20 ppm
B	8.85	10.40	11.60	12.60
C	8.65	10.10	11.50	11.80
D	8.70	10.20	11.30	12.35

Oxygen content of make-up water: 8.1 ppm

TABLE III-12. Measurements of oxygen content of diluted samples for run M-1-10337-281-B.

Sample positions	Time (min.)			
	0	5	10	15
A	8.80	9.40	10.20	10.90 ppm
B	8.65	9.45	10.10	10.60
C	8.80	9.45	10.20	10.90
D	8.35	9.50	10.30	10.70

Oxygen content of make-up water: 7.94 ppm

TABLE III-13. Measurements of oxygen content of diluted samples for run S-1-16202-1653-B.

Sample positions	Time (min.)			
	0	5	10	15
A	9.15	11.97	13.40	14.45 ppm
B	8.70	11.97	13.80	14.54
C	9.15	12.02	13.40	14.25
D	8.55	11.73	13.50	14.60

Oxygen content of make-up water: 8.45 ppm

TABLE III-14. Measurements of oxygen content of diluted samples for run S-1-10465-690-B.

Sample positions	Time (min.)			
	0	5	10	15
A	9.40	10.62	12.02	13.00 ppm
B	9.28	10.95	12.02	12.92
C	9.28	10.62	11.98	12.80
D	9.30	10.54	11.78	12.80

Oxygen content of make-up water: 8.54 ppm

TABLE III-15. Measurements of oxygen content of diluted samples for run L-1-12957-350-B.

Sample positions	Time (min.)			
	0	5	10	15
A	8.92	9.87	10.70	11.30 ppm
B	8.86	9.82	10.65	11.25
C	8.95	9.90	10.75	11.20
D	8.90	9.88	10.70	11.30

Oxygen content of make-up water: 8.41 ppm

TABLE III-16. Measurements of oxygen content of diluted samples for run M-1-18305-880-S.

Sample positions	Time (min.)			
	0	30	60	90
A	8.90	9.30	9.62	9.80 ppm
B	8.50	9.25	9.85	10.00
C	8.90	9.25	9.72	10.00
D	8.80	9.25	9.75	10.00

Oxygen content of make-up water: 8.4 ppm

TABLE III-17. Measurements of oxygen content of diluted samples for run M-1-16312-699-S.

Sample positions	Time (min.)			
	0	30	60	90
A	8.50	9.25	9.60	9.70 ppm
B	8.60	8.95	9.30	9.50
C	8.50	9.10	9.60	9.70
D	8.50	9.00	9.50	9.60

Oxygen content of make-up water: 8.5 ppm

TABLE III-18. Measurements of oxygen content of diluted samples for run S-1-16202-1653-S.

Sample positions	Time (min.)			
	0	30	60	90
A	8.70	9.10	9.50	9.70 ppm
B	8.70	9.25	9.60	9.90
C	8.90	9.20	9.60	9.80
D	8.60	9.10	9.60	9.80

Oxygen content of make-up water: 8.0 ppm

TABLE III-19. Measurements of oxygen content of diluted samples for run M-1-14321-538-S.

Sample positions	Time (min.)			
	0	30	60	90
A	8.90	9.45	9.75	9.97 ppm
B	9.00	9.40	9.80	9.84
C	9.00	9.20	9.70	9.84
D	9.05	9.40	9.70	9.87

Oxygen content of make-up water: 8.5 ppm

TABLE III-20. Measurements of oxygen content of diluted samples for run L-1-12957-350-S.

Sample positions	Time (min.)			
	0	30	60	90
A	9.20	9.55	9.82	10.05 ppm
B	9.15	9.55	9.80	10.02
C	9.22	9.62	9.91	10.10
D	9.20	9.48	9.78	10.05

Oxygen content of make-up water: 8.43 ppm

TABLE III-21. Measurements of oxygen content of diluted samples for run S-1-10465-690-S.

Sample positions	Time (min.)			
	0	30	60	90
A	9.05	9.25	9.52	9.80 ppm
B	9.09	9.30	9.52	9.70
C	9.09	9.33	9.55	9.76
D	9.02	9.25	9.45	9.72

Oxygen content of make-up water: 8.32 ppm

TABLE III-22. Measurements of oxygen content of diluted samples for run M-1-10337-281-S.

Sample positions	Time (min.)			
	0	30	60	90
A	9.17	9.32	9.65	9.94 ppm
B	9.19	9.50	9.65	9.82
C	9.16	9.42	9.66	9.88
D	9.12	9.40	9.58	9.78

Oxygen content of make-up water: 8.24 ppm

TABLE III-23. Measurements of oxygen content of diluted samples for run M-5-17712-890-B.

Sample positions	Time (min.)			
	0	5	10	15
A	9.24	11.05	12.05	12.65 ppm
B	9.22	11.20	12.10	12.60
C	9.20	11.20	12.10	12.62
D	9.17	11.00	12.05	12.55

Oxygen content of make-up water: 8.70 ppm

TABLE III-24. Measurements of oxygen content of diluted samples for run M-5-15783-707-B.

Sample positions	Time (min.)			
	0	5	10	15
A	8.98	10.25	11.35	11.90 ppm
B	9.04	10.25	11.22	11.90
C	9.02	10.30	11.22	11.90
D	8.95	10.20	11.18	11.90

Oxygen content of make-up water: 8.40 ppm

TABLE III-25. Measurements of oxygen content of diluted samples for run M-5-13857-544-B.

Sample positions	Time (min.)			
	0	5	10	15
A	9.50	10.40	11.45	12.15 ppm
B	9.42	10.60	11.35	12.20
C	9.40	10.40	11.35	12.00
D	9.40	10.35	11.40	11.95

Oxygen content of make-up water: 8.90 ppm

TABLE III-26. Measurements of oxygen content of diluted samples for run M-5-10002-284-B.

Sample positions	Time (min.)			
	0	5	10	15
A	9.65	10.35	10.75	11.15 ppm
B	9.60	10.30	10.75	11.05
C	9.60	10.30	10.80	11.10
D	9.60	10.35	10.82	11.05

Oxygen content of make-up water: 8.60 ppm

TABLE III-27. Measurements of oxygen content of diluted samples for run S-5-15677-1672-B.

Sample positions	Time (min.)			
	0	5	10	15
A	8.98	11.00	12.00	12.75 ppm
B	9.02	11.02	12.20	12.70
C	8.98	11.02	12.20	12.55
D	8.95	11.90	12.02	12.70

Oxygen content of make-up water: 8.55 ppm

TABLE III-28. Measurements of oxygen content of diluted samples for run S-5-10126-698-B.

Sample positions	Time (min.)			
	0	5	10	15
A	9.51	10.50	11.02	11.65 ppm
B	9.52	10.50	11.00	11.65
C	9.45	10.40	11.00	11.50
D	9.50	10.40	11.20	11.50

Oxygen content of make-up water: 8.20 ppm

TABLE III-29. Measurements of oxygen content of diluted samples for run L-5-12537-354-B.

Sample positions	Time (min.)			
	0	5	10	15
A	9.30	9.92	10.50	11.20 ppm
B	9.22	9.90	10.40	11.20
C	9.20	9.88	10.40	11.25
D	9.18	9.90	10.40	11.20

Oxygen content of make-up water: 8.40 ppm

TABLE III-30. Pool concentration for run M-0-18450-877-B.

Sample positions	Time (min.)			
	0	5	10	15
A	0.24090	0.37052	0.46525	0.52807
B	0.24090	0.37252	0.47422	0.53006
C	0.24488	0.36554	0.47023	0.51411
D	0.23292	0.35058	0.45029	0.51211
Average	0.23990	0.36479	0.46500	0.52109
s	0.005	0.01	0.01	0.009

TABLE III-31. Pool concentration for run M-0-10419-280-B.

Sample positions	Time (min.)			
	0	5	10	15
A	0.26881	0.28577	0.32066	0.34559
B	0.27081	0.29574	0.32864	0.35058
C	0.26183	0.28876	0.32066	0.34061
D	0.26483	0.29574	0.32964	0.35058
Average	0.26657	0.29150	0.32490	0.34684
s	0.004	0.005	0.005	0.005

TABLE III-32. Pool concentration for run S-0-16331-1648-B.

Sample positions	Time (min.)			
	0	5	10	15
A	0.24434	0.40388	0.50395	0.57040
B	0.25132	0.41385	0.51356	0.57339
C	0.24933	0.39391	0.50658	0.59333
D	0.24434	0.39092	0.51057	0.58835
Average	0.24733	0.40064	0.50867	0.58137
s	0.004	0.01	0.004	0.01

TABLE III-33. Pool concentration for run S-0-10548-688-B.

Sample positions	Time (min.)			
	0	5	10	15
A	0.26283	0.34659	0.41439	0.46624
B	0.25087	0.33462	0.42536	0.45926
C	0.25884	0.33462	0.40841	0.45926
D	0.26283	0.32465	0.40442	0.44431
Average	0.25884	0.33512	0.41315	0.45727
s	0.006	0.009	0.009	0.009

TABLE III-34. Pool concentration for run L-0-13060-349-B.

Sample positions	Time (min.)			
	0	5	10	15
A	0.24280	0.28667	0.32257	0.37442
B	0.24479	0.27969	0.32456	0.35946
C	0.24479	0.28268	0.31459	0.34849
D	0.24280	0.28468	0.32257	0.35946
Average	0.24380	0.28343	0.32107	0.36046
s	0.001	0.003	0.004	0.01

TABLE III-35. Pool concentration for run M-1-18305-880-B.

Sample positions	Time (min.)			
	0	5	10	15
A	0.27810	0.55135	0.68797	0.73001
B	0.26759	0.55135	0.69848	0.71950
C	0.25708	0.51141	0.69848	0.77205
D	0.24657	0.50931	0.61441	0.76154
Average	0.26234	0.53086	0.67484	0.74578
s	0.01	0.02	0.04	0.03

TABLE III-36. Pool concentration for run M-1-16312-699-B.

Sample positions	Time (min.)			
	0	5	10	15
A	0.28721	0.51842	0.59198	0.71810
B	0.29772	0.52892	0.64453	0.70759
C	0.28721	0.47638	0.58147	0.66555
D	0.28721	0.46587	0.62351	0.67606
Average	0.28984	0.49740	0.61037	0.69183
s	0.005	0.03	0.03	0.03

TABLE III-37. Pool concentration for run M-1-14321-538-B.

Sample positions	Time (min.)			
	0	5	10	15
A	0.23693	0.42611	0.51018	0.61528
B	0.26321	0.42611	0.55222	0.65732
C	0.24219	0.39458	0.54171	0.57324
D	0.24744	0.40509	0.52069	0.63104
Average	0.24744	0.41297	0.53120	0.61922
s	0.01	0.02	0.02	0.04

TABLE III-38. Pool concentration for run M-1-10337-281-B.

Sample positions	Time (min.)			
	0	5	10	15
A	0.27113	0.33418	0.41826	0.49183
B	0.25536	0.33944	0.40775	0.46030
C	0.27113	0.33944	0.41826	0.48183
D	0.22383	0.34469	0.42877	0.47081
Average	0.25536	0.33944	0.41826	0.47869
s	0.02	0.004	0.009	0.02

TABLE III-39. Pool concentration for run S-1-16202-1653-B.

Sample positions	Time (min.)			
	0	5	10	15
A	0.26592	0.56229	0.71258	0.82293
B	0.21863	0.56229	0.75461	0.83238
C	0.26592	0.56754	0.71258	0.80191
D	0.20286	0.53707	0.72309	0.83869
Average	0.23833	0.55730	0.72572	0.82398
s	0.03	0.01	0.02	0.02

TABLE III-40. Pool concentration for run S-1-10465-690-B.

Sample positions	Time (min.)			
	0	5	10	15
A	0.28478	0.41300	0.56103	0.66313
B	0.27217	0.44768	0.56013	0.65472
C	0.27217	0.41300	0.55593	0.64211
D	0.27428	0.40459	0.53491	0.64211
Average	0.27585	0.41957	0.55278	0.65052
s	0.006	0.02	0.01	0.01

TABLE III-41. Pool concentration for run L-1-12957-350-B.

Sample positions	Time (min.)			
	0	5	10	15
A	0.24504	0.34488	0.43211	0.49517
B	0.23874	0.33963	0.42686	0.48991
C	0.24819	0.34804	0.43737	0.48466
D	0.24294	0.34593	0.43211	0.49517
Average	0.24373	0.34462	0.43211	0.49123
s	0.004	0.004	0.004	0.005

TABLE III-42. Pool concentration for run M-1-18305-880-S.

Sample positions	Time (min.)			
	0	30	60	90
A	0.24376	0.28580	0.31943	0.33835
B	0.20173	0.28055	0.34360	0.35937
C	0.24376	0.28055	0.32994	0.35937
D	0.23325	0.28055	0.33309	0.35937
Average	0.23063	0.28186	0.33152	0.35412
s	0.02	0.003	0.01	0.01

TABLE III-43. Pool concentration for run M-1-16312-699-S.

Sample positions	Time (min.)			
	0	30	60	90
A	0.19349	0.27231	0.30910	0.31961
B	0.20400	0.24078	0.27757	0.29859
C	0.19349	0.25655	0.30910	0.31961
D	0.19349	0.24604	0.29859	0.30910
Average	0.19612	0.25392	0.29859	0.31173
s	0.005	0.01	0.01	0.01

TABLE III-44. Pool concentration for run S-1-16202-1653-S.

Sample positions	Time (min.)			
	0	30	60	90
A	0.25568	0.29772	0.33975	0.36077
B	0.25568	0.31348	0.35026	0.38179
C	0.27670	0.30822	0.35026	0.37128
D	0.24517	0.29772	0.35026	0.37128
Average	0.25831	0.30429	0.34763	0.37128
s	0.01	0.008	0.005	0.009

TABLE III-45. Pool concentration for run M-1-14321-538-S.

Sample positions	Time (min.)			
	0	30	60	90
A	0.23553	0.29333	0.32486	0.34798
B	0.24604	0.28808	0.33012	0.33432
C	0.24604	0.26706	0.31961	0.33432
D	0.25129	0.28808	0.31961	0.33747
Average	0.24473	0.28414	0.32355	0.33852
s	0.007	0.01	0.005	0.006

TABLE III-46. Pool concentration for run L-1-12957-350-S.

Sample positions	Time (min.)			
	0	30	60	90
A	0.27282	0.30961	0.33798	0.36215
B	0.26757	0.30961	0.33588	0.35900
C	0.27492	0.31696	0.34744	0.36741
D	0.27282	0.30225	0.33378	0.36215
Average	0.27203	0.30961	0.33877	0.36268
s	0.003	0.006	0.006	0.003

TABLE III-47. Pool concentration for run S-1-10465-690-S.

Sample positions	Time (min.)			
	0	30	60	90
A	0.26611	0.28713	0.31551	0.34494
B	0.27032	0.29239	0.31551	0.33443
C	0.27032	0.29554	0.31866	0.34073
D	0.26296	0.28713	0.30815	0.33653
Average	0.26743	0.29005	0.31445	0.33916
s	0.004	0.004	0.004	0.005

TABLE III-48. Pool concentration for run M-1-10337-281-S.

Sample positions	Time (min.)			
	0	30	60	90
A	0.28531	0.30108	0.33576	0.36624
B	0.28741	0.31999	0.33576	0.35362
C	0.28426	0.31159	0.33681	0.35993
D	0.28006	0.30948	0.32840	0.34942
Average	0.28426	0.31054	0.33418	0.35730
s	0.003	0.008	0.004	0.007

TABLE III-49. Pool concentration for run M-5-17712-890-B.

Sample positions	Time (min.)			
	0	5	10	15
A	0.33160	0.62785	0.79153	0.88973
B	0.32832	0.65240	0.79971	0.88155
C	0.32505	0.65240	0.79771	0.88482
D	0.32014	0.61967	0.79153	0.87337
Average	0.32628	0.63808	0.79562	0.88237
s	0.005	0.02	0.005	0.007

TABLE III-50. Pool concentration for run M-5-15783-707-B.

Sample positions	Time (min.)			
	0	5	10	15
A	0.32976	0.53763	0.71767	0.80769
B	0.33958	0.53763	0.69639	0.80769
C	0.33630	0.54581	0.69639	0.80769
D	0.32485	0.52944	0.68984	0.80769
Average	0.33262	0.53763	0.70007	0.80769
s	0.007	0.007	0.01	0

TABLE III-51. Pool concentration for run M-5-13857-544-B.

Sample positions	Time (min.)			
	0	5	10	15
A	0.34701	0.49432	0.66618	0.78075
B	0.33391	0.52705	0.64981	0.78893
C	0.33064	0.49432	0.64981	0.75620
D	0.33064	0.48613	0.65799	0.74802
Average	0.33555	0.50046	0.65595	0.76848
s	0.008	0.02	0.008	0.02

TABLE III-52. Pool concentration for run M-5-10002-284-B.

Sample positions	Time (min.)			
	0	5	10	15
A	0.41227	0.52685	0.59232	0.65779
B	0.40409	0.51866	0.49232	0.64142
C	0.40409	0.51866	0.60050	0.64961
D	0.40409	0.52685	0.60378	0.64142
Average	0.40164	0.52276	0.59723	0.64756
s	0.004	0.004	0.006	0.008

TABLE III-53. Pool concentration for run S-5-15677-1672-B.

Sample positions	Time (min.)			
	0	5	10	15
A	0.30940	0.64002	0.80370	0.92646
B	0.31594	0.64330	0.83644	0.91828
C	0.30940	0.64330	0.83644	0.89372
D	0.30449	0.62366	0.80698	0.91828
Average	0.30981	0.63757	0.82089	0.91419
s	0.005	0.009	0.02	0.01

TABLE III-54. Pool concentration for run S-5-10126-698-B.

Sample positions	Time (min.)			
	0	5	10	15
A	0.44365	0.60569	0.69080	0.79392
B	0.44529	0.60569	0.68753	0.79392
C	0.43383	0.58932	0.68753	0.76937
D	0.44201	0.58932	0.72026	0.76937
Average	0.44120	0.59751	0.69653	0.78165
s	0.005	0.009	0.02	0.01

TABLE III-55. Pool concentration for run L-5-12537-354-B.

Sample positions	Time (min.)			
	0	5	10	15
A	0.38213	0.48361	0.57854	0.69312
B	0.36904	0.48034	0.56218	0.69312
C	0.36576	0.47706	0.56218	0.70130
D	0.36249	0.48034	0.56218	0.69312
Average	0.36986	0.48034	0.56627	0.69517
s	0.009	0.003	0.008	0.004

TABLE III-56. Values of TTF for absorption in water.

Run Numbers	TTF (ml/min)	95% Confidence Limits	Coefficient of Correlation
001	1319	$\pm 7.2\%$	0.991
002	319	$\pm 8.8\%$	0.989
003	1652	$\pm 5.6\%$	0.995
004	878	$\pm 7.5\%$	0.991
005	449	$\pm 7.6\%$	0.992

TABLE III-57. Values of TTF for absorption in 5% brine.

Run Numbers	TTF (ml/min)	95% Confidence Limits	Coefficient of Correlation
501	4794	$\pm 3.3\%$	0.998
502	3314	$\pm 3.5\%$	0.998
503	2775	$\pm 7.6\%$	0.992
504	1489	$\pm 6.9\%$	0.992
505	5599	$\pm 6.3\%$	0.994
506	2543	$\pm 6.5\%$	0.994
507	1813	$\pm 10.7\%$	0.985

TABLE III-58. Values of TTF for absorption in 1% brine.

Run Numbers	TTF (ml/min)	95% Confidence Limits	Coefficient of Correlation
101	3086	$\pm 11.9\%$	0.977
102	2362	$\pm 11.0\%$	0.980
103	1889	$\pm 10.2\%$	0.984
104	979	$\pm 8.5\%$	0.989
105	4065	$\pm 6.2\%$	0.994
106	1960	$\pm 5.2\%$	0.996
107	1108	$\pm 4.2\%$	0.997

TABLE III-59. Values of TFS for absorption in 1% brine.

Run Numbers	TTF (ml/min)	95% Confidence Limits	Coefficient of Correlation
101	85	$\pm 14.4\%$	0.967
102	79	$\pm 17.7\%$	0.947
103	65	$\pm 13.9\%$	0.969
104	49	$\pm 10.9\%$	0.982
105	79	$\pm 12.0\%$	0.977
106	46	$\pm 8.2\%$	0.990
107	62	$\pm 8.3\%$	0.989

TABLE III-60. Calculated values of TF for absorption in water.

Run Numbers	TTF	TFS* (ml/min)	TF	Deviation of TF values
001	1319	117	1202	+ 103 (8.6%)
002	319	70	249	+ 33 (13.2%)
003	1652	105	1547	+ 99 (6.4%)
004	878	71	807	+ 71 (8.8%)
005	449	86	363	+ 40 (11.0%)

$$TFS = 0.0154 N_{Re}^{0.91} \pm 6.6\%, \text{ from Hauxwell (8).}$$

TABLE III-61. Calculated values of TF for absorption in 1% brine.

Run Numbers	TTF	TFS (ml/min)	TF	Deviation of TF values
101	3086	85	3001	+ 379 (12.6%)
102	2362	79	2283	+ 274 (12.0%)
103	1889	65	1824	+ 202 (11.0%)
104	979	49	930	+ 86 (9.2%)
105	4065	79	3986	+ 261 (6.5%)
106	1960	46	1914	+ 106 (5.5%)
107	1108	62	1046	+ 52 (5.0%)

TABLE III-62. Values of TF for absorption in water, from Hauswell (8).

JET	$N_{Re}$	$N_{We}$	TF (ml/min)	Deviation
XS	4083	157	93	$\pm$ 6.4%
S	5177	157	112	$\pm$ 10.1%
S	8461	421	504	$\pm$ 3.3%
S	11409	765	1420	$\pm$ 9.9%
M	8020	157	181	$\pm$ 6.3%
M	9000	198	320	$\pm$ 7.7%
M	17675	765	2060	$\pm$ 4.0%
M	20000	979	2857	$\pm$ 6.2%
L	19834	765	2324	$\pm$ 4.7%

TABLE III-63. Calculated values of TF for absorption in 5% brine.

Run Numbers	TTF	TFS* (ml/min)	TF	Deviation of TF values
501	4794	84	4710	$\pm$ 168 (3.6%)
502	3314	74	3240	$\pm$ 125 (3.9%)
503	2775	64	2711	$\pm$ 219 (8.1%)
504	1489	45	1444	$\pm$ 108 (7.5%)
505	5599	73	5526	$\pm$ 362 (6.6%)
506	2543	46	2497	$\pm$ 171 (6.8%)
507	1813	58	1755	$\pm$ 201 (11.5%)

\* Calculated values, see Figure 8, for correlation.

TABLE III-64. Measurements of oxygen content for Run number  $\frac{1}{2}$  01.  
Run condition M- $\frac{1}{2}$ -18414-879-B.

Sample positions	Time (min.)			
	0	5	10	15
A	8.71	10.90	12.55	13.15 ppm
B	8.77	11.05	12.61	13.15
C	8.70	10.99	12.62	13.00
D	8.64	10.90	12.35	13.00

Oxygen content of make-up water: 8.60 ppm

TABLE III-65. Measurements of oxygen content for Run number 201.  
Run condition M-2-18162-882-B.

Sample positions	Time (min.)			
	0	5	10	15
A	8.90	11.35	12.55	13.60 ppm
B	8.88	11.30	12.55	13.60
C	8.92	11.35	12.50	13.65
D	8.90	11.35	12.55	13.60

Oxygen content of make-up water: 8.00 ppm

TABLE III-66. Pool concentration for run M- $\frac{1}{2}$ -18414-879-B.

Sample position	Time (min.)			
	0	5	10	15
A	0.20683	0.43119	0.60022	0.66169
B	0.21298	0.44655	0.60637	0.66169
C	0.20581	0.44041	0.60739	0.64632
D	0.19966	0.43119	0.57973	0.64632
Average	0.20632	0.43734	0.59843	0.65401
s	0.005	0.008	0.01	0.009

TABLE III-67. Pool concentration for run M-2-18162-882-B.

Sample positions	Time (min.)			
	0	5	10	15
A	0.27970	0.54896	0.68084	0.79623
B	0.27750	0.54346	0.68084	0.79623
C	0.28190	0.54896	0.67534	0.80173
D	0.27970	0.54896	0.68084	0.79623
Average	0.2797	0.54759	0.67947	0.79761
s	0.002	0.003	0.003	0.003

TABLE III-68. Values of TTF for absorption in  $\frac{1}{2}$ % and 2% brine.

Run Numbers	TTF (ml/min)	95% Confidence Limits	Coefficient of Correlation
$\frac{1}{2}$ 01	2441	$\pm 9.6$	0.985
201	3425	$\pm 3.3\%$	0.998

TABLE III-69. Calculated values of TF for absorption in  $\frac{1}{2}$ % and 2% brine.

Run Numbers	TTF	TFS* (ml/min)	TF	Deviation of TF values
$\frac{1}{2}$ 01	2441	87	2354	$\pm 245$ (10.4%)
201	3425	86	3339	$\pm 124$ ( 3.7%)

\*Calculated values, see Figure 8 for correlation.

## APPENDIX IV

Sample Calculations

To illustrate the calculations in this work, Run 105 was used in this section. Data for Run 105, Run conditions S-1-16202-1653-B and S-1-16202-1653-S were tabulated in Table III-13 and III-18. They were used to determine the TTF and TFS respectively.

For each run, 16 samples were collected. They belong to 4 different time intervals with 4 samples in each group.

Every single sample can be designated by position and time, C (position, time). To determine the TTF, C (D, 10) of Table III-13 was used as an example.

$$C (D, 10) = 13.5 \text{ ppm}$$

First of all, the reading was corrected for salinity effect according to owner's manual. At 20°C the following equation was used:

$$\text{correction factor} = 1.0 - \left( \frac{\text{Chlorinity of sample}}{20000 \text{ mg/l Cl}^-} \right) \left( \frac{9.2 - 7.4}{9.2} \right) \quad (\text{IV-1})$$

where

$$\begin{aligned} \text{chlorinity of sample} &= \frac{\left( \text{chlorinity of original sample} \right) * \left( \text{volume of original sample} \right)}{\left( \text{volume of diluted sample} \right)} \quad (\text{IV-2}) \\ &= \frac{(6127 \text{ ppm Cl}^-) (125 \text{ ml})}{550 \text{ ml}} \\ &= 1392.5 \text{ mg/l Cl}^- \end{aligned}$$

This correction was used to compensate the effect of salinity. A simple mass balance was used to calculate the ppm of the original pool sample.

$$\text{Actual ppm} = \frac{\left( \begin{array}{c} \text{Diluted} \\ \text{sample} \\ \text{ppm} \end{array} \right) * 550 \text{ ml} - \left( \begin{array}{c} \text{Make-up} \\ \text{water} \\ \text{ppm} \end{array} \right) * 425 \text{ ml}}{125 \text{ ml}}$$

For Table III-13 make-up water ppm = 8.45.

Substituting all the values into the equations, the actual ppm of C (D, 10) = 29.86084.

From Table III-2, solubility of oxygen in brine (6127 ml/l Cl<sup>-</sup>, 1% NaCl, in water) exposed to water saturated air at 760 mm Hg was found to be 8.60984 ppm. This solubility was converted to the experimental conditions according to the following equation:

$$\begin{aligned} \text{Actual solubility} &= 8.60984 \text{ ppm} * \left( \frac{765 \text{ mm Hg}}{760 \text{ mm Hg}} \right) * \left( \frac{99.59\% \text{ pure } O_2}{20.9\% O_2 \text{ in air}} \right) \\ &= 41.29642 \text{ ppm} \end{aligned}$$

Then the dimensionless concentration, C<sup>+</sup>, was computed.

$$\begin{aligned} C^+ (D, 10) &= \left( \frac{\text{actual ppm}}{\text{actual solubility}} \right) = \frac{29.86084}{41.29642} \\ &= 0.72309 \end{aligned}$$

The value of C<sub>0</sub><sup>+</sup> was computed by averaging all the values of C<sup>+</sup> at time = 0. In this run, C<sub>0</sub><sup>+</sup> = 0.23833

Then values of  $\ln(z)$  were calculated

$$\begin{aligned} \ln [z(D, 10)] &= \ln \left[ \frac{1 - C_0^+}{1 - C^+(D, 10)} \right] \\ &= \ln \left[ \frac{1 - 23833}{1 - 0.72309} \right] \\ &= 1.01180 \end{aligned}$$

Subroutine RLONE in International Mathematical and Statistical Library was used to calculate the slope of  $\ln(z)$  vs time through the origin (see Figure IV-1). The slope of this line was found to be  $0.09991 \text{ min}^{-1}$ .

Recall Equation (16)

$$\ln(z) = \left( \frac{\text{TTF}}{V} \right) (\text{time})$$

That is

$$\begin{aligned} \text{TTF} &= (\text{slope}) (V) = (0.09991) (40689) \\ &= 4065 \text{ ml/min.} \end{aligned}$$

The coefficient of correlation,  $R$ , was found to be 0.994.

The following equation was used to calculate the 95% confidence limits, CL.

$$\text{CL} = \pm \frac{(t_{0.025}^{\text{df}})}{\sqrt{N-2}} * \frac{s_{y,x}}{s_x} * \frac{100\%}{\text{slope}} \quad (\text{IV-4})$$

But

$$s_{y,x} = s_y \sqrt{1 - R^2} \quad (\text{IV-5})$$

Therefore

$$CL = \pm \left( \frac{t_{0.0025}^{df}}{\sqrt{N-2}} \right) \left( \frac{s_y}{s_x} \right) \left( \sqrt{\frac{1-R^2}{\text{slope}}} \right) \times 100\% \quad (\text{IV-6})$$

where

df = degree of freedom

N = number of sample points

$s_x$  = standard deviation of x

$s_y$  = standard deviation of y

$s_{y,x}$  = standard error of estimate of y or x

t = value of student's t distribution

Substituting the appropriate values into Equation (IV-6).

$$\begin{aligned} CL &= \pm \frac{2.14}{\sqrt{16-2}} * \frac{0.56721}{5.77350} * \sqrt{\frac{1-0.99389^2}{0.09991}} \times 100\% \\ &= \pm 6.2\% \end{aligned}$$

Then

$$TTF = 4065 \pm 6.2\% \text{ ml/min}$$

or

$$TTF = 4065 \pm 252 \text{ ml/min}$$

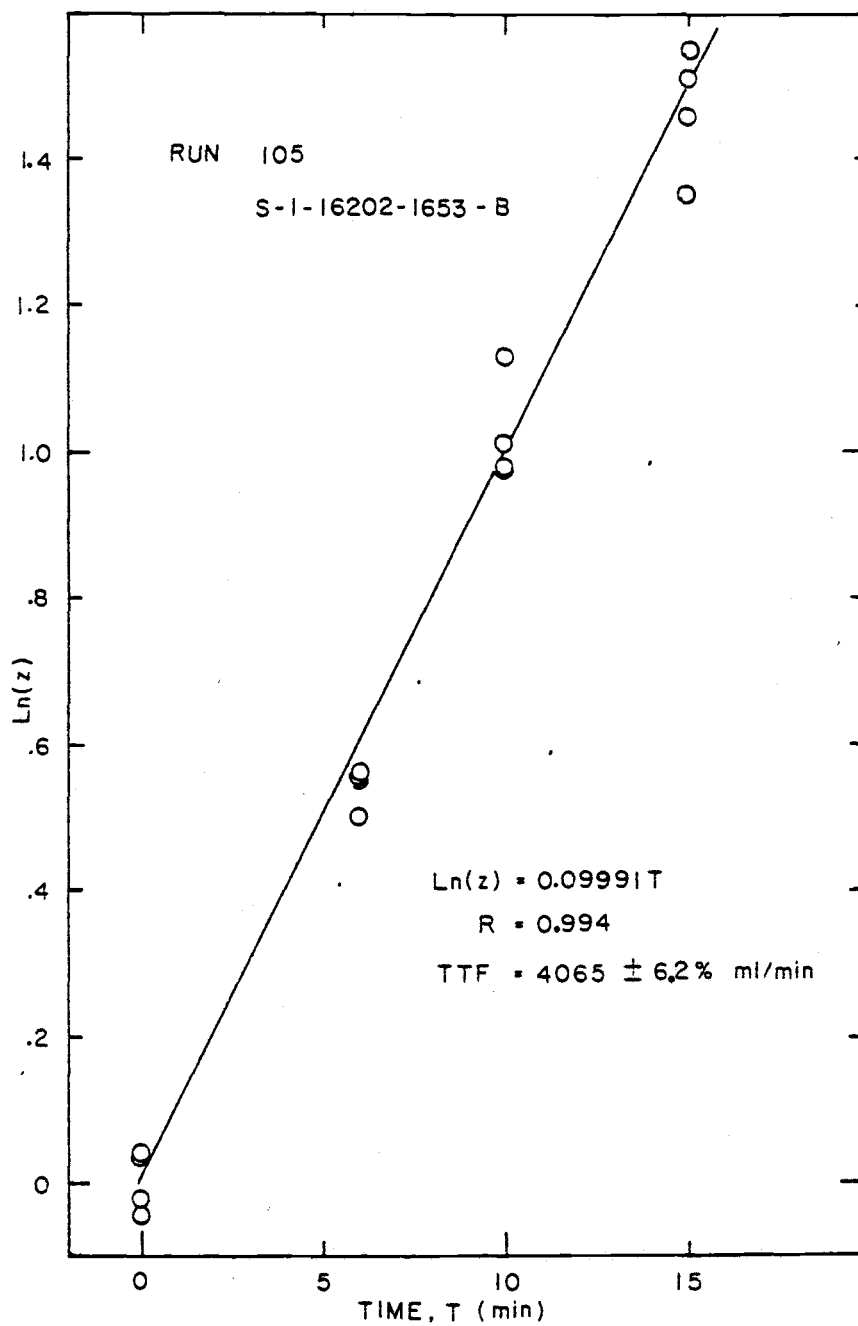


FIGURE IV-1. Determination of TTF

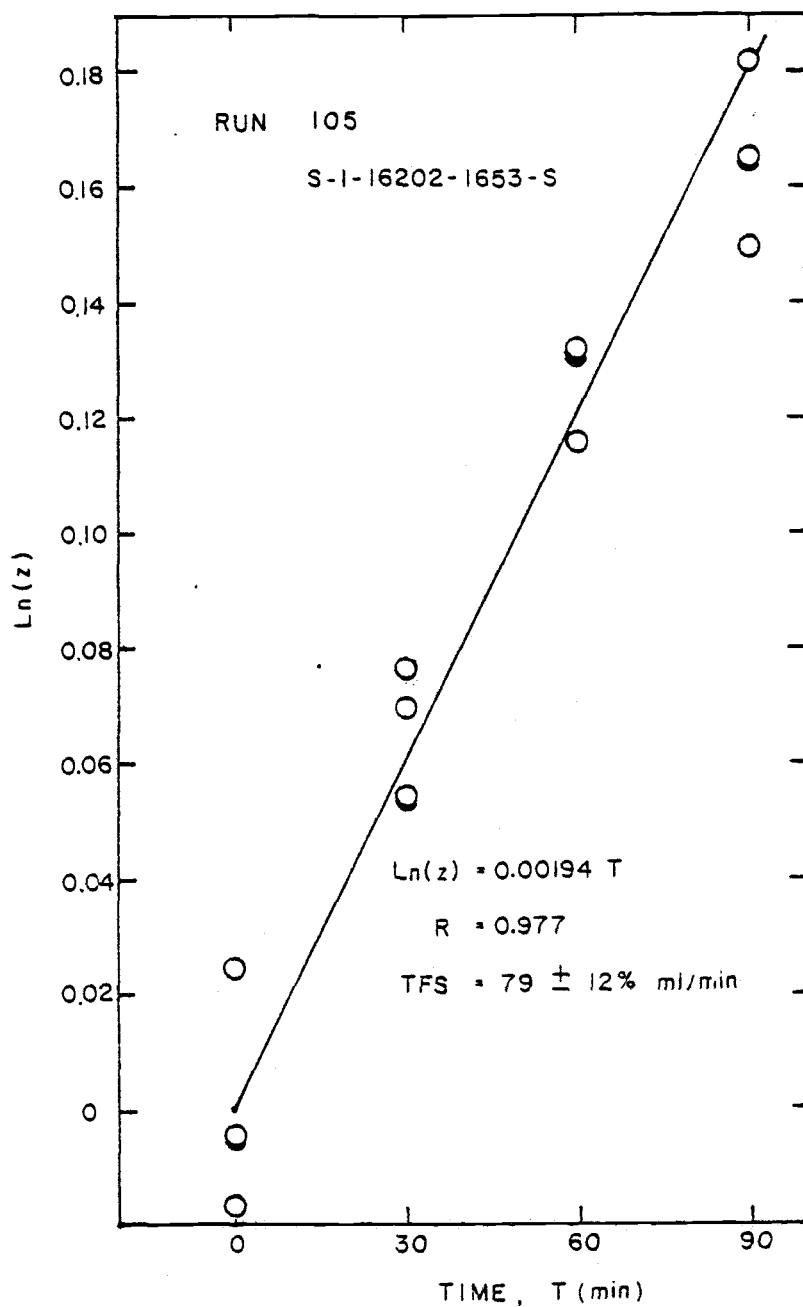


FIGURE IV-2. Determination of TFS.

Similarly, TFS was calculated:

$$\text{TFS} = 79 \pm 12.0\% \text{ ml/min}$$

or

$$\text{TFS} = 79 \pm 9 \text{ ml/min}$$

Recall Equation (11)

$$\text{TF} = \text{TTF} - \text{TFS}$$

Therefore,

$$\begin{aligned} \text{TF} &= (4065 \pm 252) - (79 \pm 9) \frac{\text{ml}}{\text{min}} \\ &= 3986 \pm 261 \frac{\text{ml}}{\text{min}} \end{aligned}$$

or

$$\text{TF} = 3986 \pm 6.5\% \frac{\text{ml}}{\text{min}}$$